Modulation of T cell activation and function by PI3K-controlled transcriptional regulators Foxo1 and Id3.

Jenna Marie Sullivan

A dissertation submitted in partial fulfillment
of the requirements for the degree of

Doctor of Philosophy

University of Washington
2018

Reading Committee:

Daniel J. Campbell, Chair
Pamela J. Fink
Kevin B. Urdahl

Program Authorized to Offer Degree:

Department of Immunology

University of Washington

Abstract:

Modulation of T cell activation and function by PI3K-controlled transcriptional regulators Foxo1 and Id3.

Jenna Marie Sullivan

Chair of the Supervisory Committee:
Associate Professor Daniel J. Campbell
Department of Immunology

αβ T cells are a diverse population of cells which help to mediate both inflammation and tolerance. T cells can be broadly divided based on their localization, activation, and expression of transcription factors into naïve, effector, memory and regulatory T cells. Conventional $CD4^+$ and $CD8^+$ T cells mediate inflammation and immune memory, helping to clear viral, bacterial and parasitic infections. $Foxp3^+$ regulatory T cells (T_R) are potent regulators of tolerance by preventing auto-reactive effector function and dampening immune responses after infection. Although diverse in their function and localization, all αβ T cells are regulated by the phosphoinositide 3-kinase (PI3K) signaling cascade. In T cells, the PI3K pathway can be activated or inhibited by a variety of signals, including T cell receptor (TCR) stimulation, cytokines, growth factors, costimulatory receptors and coinhibitory receptors. In both $CD4^+$ and $CD8^+$ T cells, varied strength and duration of PI3K signaling can instruct cells towards effector function, memory phenotypes, anergy or exhaustion. These observations demonstrate the essential role of PI3K signaling in regulating the complex pathways T cells must follow for appropriate responses to an immune threat. In this work we highlight two proteins, Forkhead

box O (Foxo) family member, Foxo1 and inhibitor of DNA binding protein (Id), Id3, which help regulate T cell function downstream of PI3K signaling.

Herein, we demonstrate that Foxo1 regulates T cell homeostasis starting at thymic development and plays a vital role in regulating effector T cell differentiation and function. Using several transgenic mouse models, we prevented inactivation of Foxo1 in T cells, resulting in both $CD4^+$ and $CD8^+$ T cells which have constitutively active of Foxo1 ($Foxo1^{CA}$). Foxo1 activation in the thymus prior to positive-selection resulted in decreased thymic output of mature CD4 single positive T cells and development of spontaneous autoimmunity associated with autoreactive B cells. Conversely, constitutive activation of Foxo1 after thymic maturation yielded healthy mice with a naïve-skewed T cell population, in which T cells were defective in effector function. RNA-seq analysis of stimulated control versus $Foxo1^{CA}$ $CD8^+$ T cells highlighted several key pathways regulated by Foxo1. We show that during TCR stimulation, inactivation of Foxo1 allows for coordinated changes in costimulatory receptors, inhibitory receptors and key transcription factors. Examining regulation of inhibitors of DNA binding (Id) proteins in T_R, we show that dynamic downregulation of Id3 by PI3K signaling helps define three distinct T_R populations, $Id3^+CD62L^{hi}CD44^{lo}$ central (c)T_R, $Id3^+CD62L^{lo}CD44^{hi}$ effector (e)T_R and $Id3^-$ eT_R. We further go on to show that $Id3^-$ eT_R are highly enriched in non-lymphoid tissues and have a tissue-resident T_R molecular signature. Together our findings add to the known functions of PI3K regulation in αβ T cell homeostasis, differentiation and function.

Table of Contents

Dedication

For my parents, who taught me the value of hard work, encouraged me to explore and gave me their unconditional love and support.

Acknowledgements:

We would like to thank K. Arumuganathan (Aru) and Tuan Nguyen for help with flow cytometry and cell sorting. Vivian Gersuk and the BRI Genomics Core for running RNA-seq samples. Drs. Ananda Goldrath, Ming Li, Mohamed Oukka and Estelle Bettelli provided Id3-GFP, Foxo1^{CA}, Ai6, dLck-cre mice respectively. We thank Dr. Pamela Fink for generously providing RIP-mOVA mice and VSV-OVA. We thank Dr. Jeffery Duggan, Kristen Mittelsteadt and Joanna Maltbaek for help with experiments. Samantha Motley and McKenna Shreve provided laboratory support and helped maintain animal colonies. Dr. Andrew Burich, Carlos Toledano and the BRI vivarium staff for care and maintenance of animal colonies. We thank Drs. Pamela Fink, Kevin Urdahl, David Rawlings and Jessica Hamerman for their comments and suggestions regarding the data and experiments herein. Our most heartfelt thanks to Barbara Höllbacher for analyzing RNA-seq data and providing instrumental insight into experiments. We also thank members of the Campbell Lab for their support and helpful discussions.

List of Figures

Chapter 1:

Introduction

Immune Tolerance

A key feature of the immune system is recognition of 'self' versus 'non-self' antigens. Establishing immune tolerance to 'self' is an essential process to prevent autoimmunity. Immune tolerance is established by two mechanisms, central and peripheral tolerance. Central tolerance is established during positive or negative selection in the thymus, with deletion of most autoreactive T cells. Although an efficient process, central tolerance does not eliminate all self-reactive T cells, due to some escape and the insurmountable task of presenting all 'self' peptides in the thymus (1, 2). As such, outside the thymus, peripheral tolerance helps to eliminate or dampen autoreactive responses through a variety of processes. A key peripheral tolerance pathway to eliminate auto-reactive T cells is through TCR:MHC interactions which can result in anergy, exhaustion and/or death. Downstream of TCR:MHC interactions is the phosphoinositide 3-kinase (PI3K) signaling cascade that regulates T cell survival, proliferation, function and localization (3, 4). In this dissertation, we explore various mechanism by which PI3K signaling regulates peripheral tolerance.

Conventional T cells

After maturation, single positive $CD4^+$ and $CD8^+$ T cells exit the thymus as naïve $CD44^{lo}$ $CD62L^{hi}$ T cells. Naïve T cells circulate through the body via blood and lymph sampling peptides presented by antigen presenting cells (APCs), scanning for peptides recognized by their TCR. Primary activation of naïve T cells is controlled by coordination of three signals. Signal 1 is provided by TCR engagement with peptide presented on MHC molecules, which promotes activation and engagement of the various downstream signaling cascades including PI3K,

Mek/Erk, mTOR and NFAT. Signal 2 is provided by signaling through costimulatory receptors such as CD28, ICOS and OX40 by ligands on APCs. These costimulatory signal help promote survival and proliferation. Lastly, cytokines often act as signal 3, providing guidance for lineage differentiation. Together these signals promote differentiation and commitment to effector phenotypes through altered gene expression and chromatin remodeling.

Effector $CD8^+$ T cells, referred to as cytotoxic T lymphocytes (CTL), are efficient killers of pathogen-bearing target cells. After activation, effector $CD8^+$ T cells mediate immune responses to pathogens through release of pore-forming granzymes and perforins, and inflammatory cytokines IFNɣ and TNFα (5). Expression of IL-7R (CD127) and KLRG1 can be used to broadly divide effector $CD8^+$ T cells with differing memory potential; $KLRG1^{hi}$ $IL\text{-}7R^{lo}$ short-lived or terminal effector cells (T_{eff}) and $KLRG1^{lo}$ $IL\text{-}7R^{hi}$ long-lived memory precursors (T_{MP}) (6). Recent studies suggest that memory $CD8^+$ T cells arise mainly from the T_{MP} population rather than deriving directly from naïve $CD8^+$ T cells (7, 8). Memory $CD8^+$ T cells can be subdivided in three populations: central memory (T_{CM}), effector memory (T_{EM}) and tissue resident memory (T_{RM}) (9). Although all long-lived memory populations, these distinct subsets have unique localization, surveillance, reactivation and molecular profiles. T_{CM} and T_{EM} are found primarily in the circulation and secondary lymphoid organs (SLO). The more recently identified T_{RM} are found in non-lymphoid tissues, providing a memory response at barrier sites. Along with their unique residency, T_{RM} express tissue homing receptors such as CCR9, CXCR6, CCR10 and tissue retention factors such as CD103 and CD69 (10, 11).

$CD4^+$ $Foxp3^-$ conventional T cells can differentiate into various T ‘helper’ subsets (Th) depending on the strength of TCR stimulation and cytokines present during activation. Although often playing a supporting role, these various flavors of Th cells allow for diverse responses to pathogens and/or promotion of autoimmunity (12). Th subets play a vital role in directing the immune response by producing cytokines. Upon infection, Th1 cells aid in clearing intracellular

bacteria by activating macrophages and Th2 cells help clear extracellular parasite by activating B cells and eosinophils. T follicular helper (Tfh) cells are essential for promoting germinal center reactions and B cell responses through their production of IL-4 and IL-21 (13, 14). Regulation of Th subsets is vital, with breaks in tolerance leading to autoimmunity and inflammation. Unchecked Th1 and Th17 cells mediate neurological damage associated with multiple sclerosis (15) and misdirected Th2 cells drive allergy and asthma (16).

Regulatory T cells

As a counter balance to conventional T cells, $CD4^+$ $Foxp3^+$ regulatory T cell (T_R) help dampen immune responses, maintain peripheral tolerance and prevent autoimmunity. The suppressive capacity of T cells was first identified by transfer of $CD4^+$ $CD25^+$ T cells and their ability to reverse inflammation in thymectomized mice (17). Foxp3 was identified as a key regulator of T_R in the scurfy mouse model, in which mutations in the *Foxp3* gene result in autoimmunity manifesting with runting, dermatitis and failure to thrive (18, 19). In humans, mutations in the *FOXP3* gene result in immunodysregulation polyendocrinopathy enteropathy X-linked syndrome (IPEX) with loss of tolerance and autoimmunity (20). T_R dampen effector T cell responses through a variety of mechanisms. T_R produce cytokines such as IL-10, IL-35 and granzyme B, which inhibitor or kill effector T cells. Additionally T_R act as a cytokine sink, sopping up available IL-2 and preventing IL-2-driven effector T cell proliferation (21). Furthermore, T_R have high expression of coinhibitory markers TIGIT, CTLA4 and LAG3, which aid in dampening effector T cell activation (22). Although T_R are vital in preventing autoimmunity, they can be detrimental to some immune responses. T_R hinder clearance of cancerous cells by preventing conventional T cell activation, thereby promoting cancer cell growth (23-25).

T_R are highly dependent on IL-2 for their survival, function and proliferation. As a mechanism to control suppression by T_R, T_R themselves do not produce IL-2. They are dependent on paracrine IL-2 from conventional T cells, thus creating a feedback loop in which activated effector T cells produce IL-2, promoting T_R which limit effector T cell pathology (25, 26). As infection and thus antigen decrease, effector T cell number and cytokine production decrease, leading to diminished IL-2 production and reduced T_R numbers. In both mice and humans, T_R express high levels of CD25, the high affinity receptor for IL-2. In mice, T_R are the predominant T cell population expressing high levels of CD25; however in humans activated T cells also upregulate CD25 providing competition for available IL-2. Modulation of T_R through treatment with IL-2 is an active area of research for many autoimmune diseases such as type I diabetes (27). A better understanding of T_R affinity for IL-2 is required to help overcome difficulties in dosing with IL-2 to prevent aberrant proliferation of effector T cells.

Most T_R are produced in the thymus, exiting as natural or thymic T_R. Additionally, in the presence of TGFβ and TCR stimulation, naïve conventional $CD4^+$ T cells can differentiate in the lymphoid periphery into $Foxp3^+$ expressing T_R also known as induced T_R. During thymic development unlike conventional T cells, T_R are selected for autoreactive TCRs, which aid in their suppression of autoreactive effector cells. Work by our lab and others have demonstrated the phenotypic and functional heterogeneity of T_R (28-32). Like conventional T cells, T_R can be divided based on expression of CD44 and CD62L into $CD44^{lo}$ $CD62L^{hi}$ central T_R (cT_R) and $CD44^{hi}$ $CD62L^{lo}$ effector T_R (eT_R). These two populations of T_R are distinct in their function, localization, dependence on IL-2 and PI3K signaling (3, 28). In the periphery, cT_R are found in SLO, are dependent on IL-2 signaling and are equipped to suppress T cell priming (28, 29). In concordance with their dependence on IL-2, cT_R express higher levels of CD25 and elevated levels of phosphorylated (p) Stat5 compared to eT_R. In contrast to cT_R, the more highly activated eT_R are found in non-lymphoid organs, suppress effector $CD4^+$ T cells and do not access IL-2,

instead relying on costimulatory signals such as ICOS for PI3K signaling (28). These two distinct subsets, cT_R and eT_R, demonstrate a division of labor among T_R which is activation, location and signaling dependent. Although PI3K-AKT-mTor signaling has been implicated in driving cT_R to eT_R transition (33), the precise mechanisms driving differentiation in T_R is not well defined.

PI3K signaling cascade

The PI3K signaling cascade is an important pathway in many cells in the immune system. PI3-kinases were first discovered in 1984 due to their association with oncogene activity of Tyr kinases in cancer and continue to be a widely studied topic. PI3K signaling regulates a wide array of cellular functions, including but not limited to, organelle trafficking, proliferation, survival, cytokine production, migration and metabolism (4, 34). PI3-kinases broadly act by phosphorylating the 3-OH group of membrane-associated inositol lipids which modulate the activity of many downstream proteins. Mammals have eight isoforms of PI3K which can be grouped into three classes. Class I PI3-kinases can be further divided into class IA and IB and are the most widely studied in T cells (3, 4, 34-36). Class I PI3-kinases are activated by cell surface receptors with class IA PI3-kinases downstream of TCR signaling and class IB PI3-kinases downstream of G-coupled protein receptors such as chemokine and cytokine receptors. In T cells, upon activation, PI3K phosphorylates PIP2 to PIP3, which recruits and activates downstream signaling components such as PDK1, AKT and mTOR.

Protein kinase B, commonly known as Akt, is a serine/threonine kinase which is important downstream regulator of the PI3K signaling cascade. Along with PDK1, Akt binds to PIP3, allowing for phosphorylation at Ser302 by PI3K. For full activation of Akt, a second phosphorylation at Ser473 by mTORC must occur. Once activated Akt mediates several cellular

functions through modulations of downstream PI3K targets such as Foxo1. Akt, along with SGK1, phosphorylates Foxo1 at three sites, resulting in its inactivation and translocation from the nucleus. Through its regulation of Foxo1, Akt activity controls pathways involved in apoptosis and cell cycle. Independent of Foxo1, Akt inhibits Bad, cMyc and HIF1α, adding additional control of cell survival and metabolism. Gain of function mutations in Akt and constitutively active forms of PI3K result in lymphocyte proliferation and autoimmunity (35).

Another serine/threonine kinase involved in the PI3K signaling cascade is mechanistic target of rapamycin (mTOR). For its function, mTOR associates with two distinct sets of proteins to form functional complexes. mTOR complex 1 (mTORC1) is defined by its association with regulatory-associated protein of mTOR (RAPTOR) and mTORC2 is known for association with RAPTOR-independent companion of TOR (RICTOR). mTOR functions both upstream and downstream of Akt, with mTORC2 phosphorylating Akt resulting in its activation and mTORC1 activation downstream of Akt signaling (37). Input from the two mTOR complexes guides $CD4^+$ Th differentiation with mTORC1 promoting Th1 and Th17 development and mTORC2 promoting Th2 cells. $CD8^+$ effector T cell function has been linked to mTORC2 through its regulation of Akt downstream Foxo1 (35). Akt/mTORC2 mediated phosphorylation of Foxo1 results in its inactivation and reduced expression of key target genes. Active Foxo1 regulates CD62L, IL-7R and CCR7expression, all key components whose expression must be downregulated to promote differentiation of effector $CD8^+$ T cells.

A key negative regulator of PI3K is phosphatase and tensin homologue (PTEN), which, through lipid phosphatase activity, dephosphorylates PIP3, converting it back to PIP2 (38). PTEN negative regulation of PI3K signaling downstream of the TCR allows for secondary signals, such as costimulatory receptors to fine tune T cell responses. Absence or inactivation of PTEN in T cells can lead to uncontrolled proliferation, resulting in autoimmunity and/or lymphomas. Given its role in regulating PI3K-mediated proliferation, PTEN is targeted for

suppression by various tumors (4, 38). PTEN is differentially expressed within the T cell compartment; relative to conventional T cells, T_R maintaining high expression of PTEN (39). Indeed, loss of PTEN specifically in T_R leads to a loss of T_R due to reduced CD25 and Foxp3 expression (40). Along with observed defects in Akt signaling and increased ICOS signaling in T_R, these data suggest that T_R are less reliant on TCR signaling for activation of PI3K targets (28, 40).

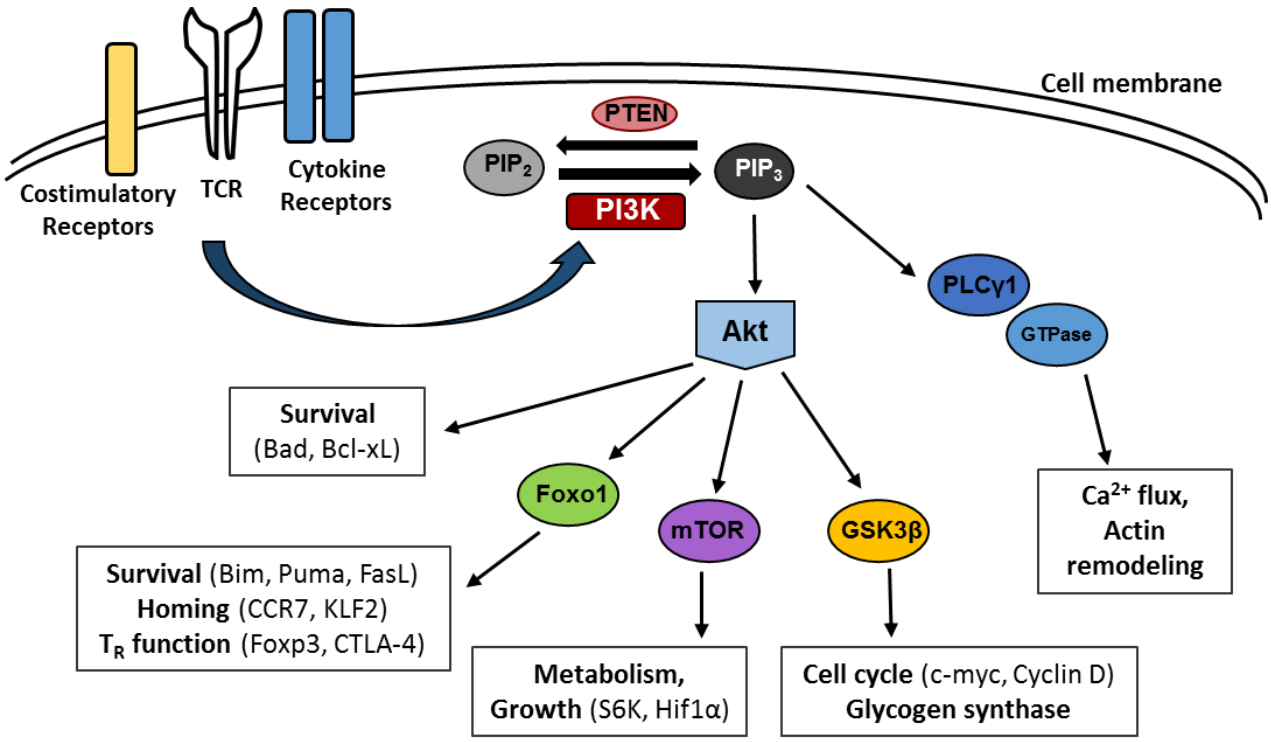

Figure 1.1 PI3K signaling cascade

PI3K are activated downstream of costimulatory receptors, TCR signaling and cytokine receptors, which recruit and activate PI3K. PI3K phosphorylates PIP2 to PIP3, which recruits and activates downstream signaling components such as PDK1, AKT and mTOR.

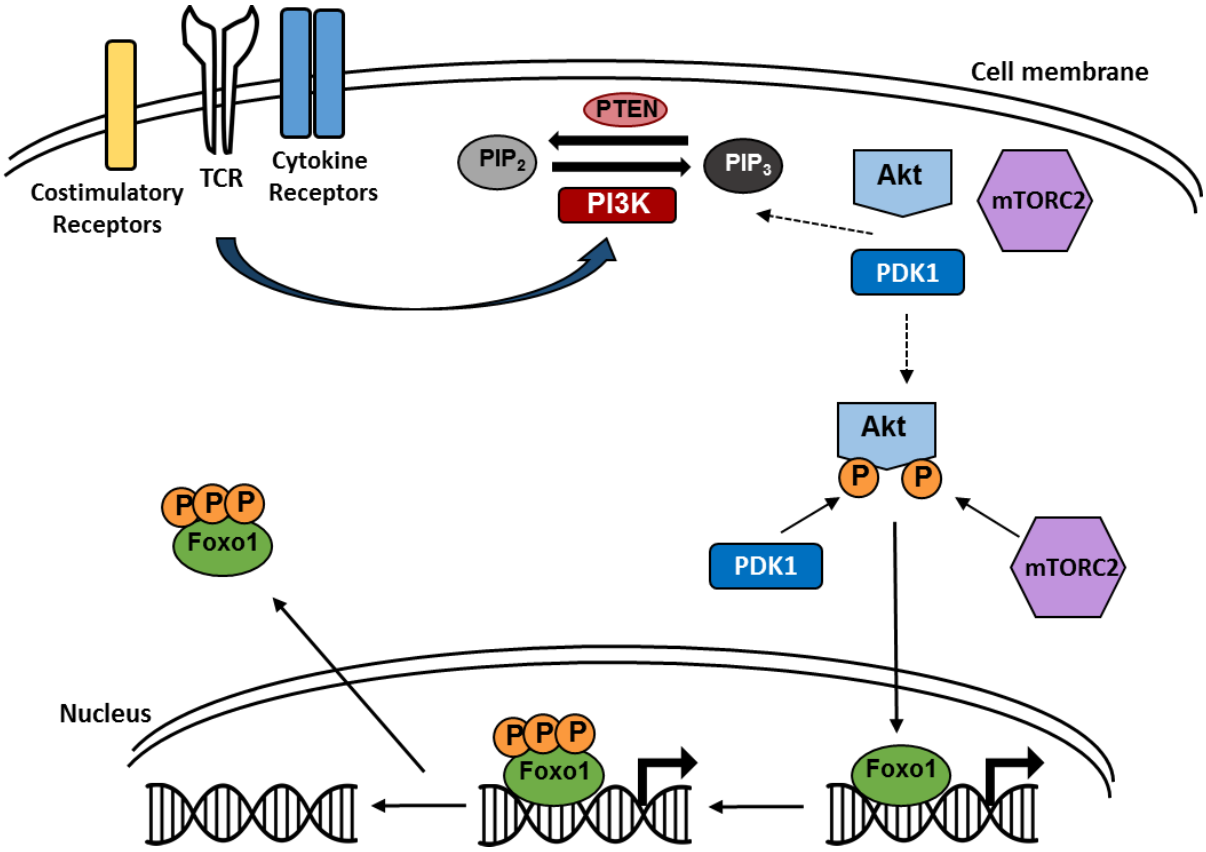

Figure 1.2 Phosphorylation and inactivation of Foxo1 downstream of PI3K

Upon engagement of PI3K signaling, PDK1 and Akt are recruited and bind to PIP3, allowing for PDK1 mediated phosphorylation of Akt at Ser302 by PI3K. For full activation of Akt, a second phosphorylation at Ser473 by mTORC must occur. Once activated Akt phosphorylates Foxo1 at three sites, resulting in its inactivation, translocation from the nucleus and loss of transcriptional regulation.

Summary and unanswered questions

Of the many proteins PI3K regulates we focused on two, Foxo1 and Id3, both of which are downregulated upon PI3K signaling in T cells. Several groups have demonstrated that active Foxo1 in the nucleus, is inactived by phosphorylation at three sites by Akt-SGK1 downstream of PI3K signaling (41). Although the mechanisms regulating Id3 are less well established, Id3 expression decreases upon engagement of TCR and PI3K signaling in both conventional and regulatory T cells (42). The precise mechanisms by which Foxo1 and Id3 regulate T cell development, homeostasis and function are areas of ongoing research. In the experiments herein, we focus on examining Foxo1 regulation of conventional T cells and Id3 regulation in T_R. In Chapter 3 we examine how dysregulated expression of Foxo1 during thymic development leads to spontaneous inflammatory disease in mice. In Chapter 4 we explore how sustained expression of Foxo1 impacts effector $CD8^+$ T cell development and function. Finally, in Chapter 5 we identify Id3 expression as a determiner of T_R tissue residency and function. A precise understanding of the PI3K signaling cascade is essential for manipulation of the immune system for therapeutics against both cancer and autoimmune diseases.

Chapter 2:

Materials and methods

Mice

C57BL/6 (B6), CD45.1^{+} B6 congenic, Foxp3.mRFP, OT-I, CD4-cre and IRF8-floxed mice were purchased from The Jackson Laboratory. Foxp3.mRFP mice have a monoallelic red fluorescent protein (mRFP) knocked in downstream of the Foxp3 gene, allowing for visualization of Foxp3 protein. OT-I transgenic mice contain transgenic inserts for TCRα-V2 and TCRβ-V5 which are specific for ovalbumin (OVA) peptide residues 257-264. Id3-GFP mice were a gift from Ananda Goldrath (UCSD, La Jolla, California) have been previously described (43). Id3-GFP mice contain an IRES-GFP knocked into the Id3 locus allowing for GFP expression when Id3 is transcribed. Foxo1^{CA} mice, in which the ROSA26 allele contains a mutated human form of Foxo1 which can not be phosphorylated, were generously provided by Ming Li (MSKCC, New York City, NY) (29, 44). Control Ai6 mice were a gift from Mohamed Oukka (SCRI, Seattle, WA), these mice contain a GFP expressing ROSA26 locus without a gene of interest and can be used to monitor cre-recombinase driven removal of stop-flox cassettes (45). Distal Lck-cre (dLck-cre) mice contain a cre-recombinase gene driven by the distal promoter of lymphocyte protein tyrosine kinase (Lck) and were provided by Estelle Bettelli (BRI, Seattle, WA). RIP-mOVA mice, in which membrane-bound ovalbumin is expressed under the rat insulin promoter in the pancreas, were a gift from Pamela Fink (UW, Seattle, WA). All mice were housed and bred at the Benaroya Research Institute (Seattle, WA) and all experiments were performed in accordance with the guidelines of the Institutional Animal Care and Use Committee of Benaroya Research Institute.

Cell isolation

Unless noted below, single cell suspensions isolated from tissues using manual disruption. Peritoneal exudate cells (PEC) isolated by injecting sterile PBS into peritoneal cavity of euthanized mice, gentle disruption to dislodge cells and collection of injected PBS. Intraepithelial lymphocytes (IEL) and lamina propria lymphocytes (LPL) were isolated from pooled large and small intestine as previous described (46). Lymphocytes were further purified by resuspension in 44% Percoll ™ (GE Healthcare) layered over 67% Percoll ™ and spun at 1,800 g for 20 mins. Lung and fat were finely minced, digested with 0.26U/mL Liberase TM (Roche) and 10U/mL DNAse (Sigma) for 1 hr at 37°C and filtered. For skin tissue, ears were processed as above with 0.14U/mL Liberase TM and 10U/mL DNAse. For lymph collection, mice were fed 20mL/kg 'Half and Half' by oral gavage and sacrificed 2-3 hrs later. Intestinal lymph collected from the cisterna chyli was directly stained for flow cytometry.

Histology and immunohistochemistry

For analysis of pathology and immune cell infiltration into nonlymphoid organs, tissue was fixed with 10% formalin, paraffin embedded, sectioned and stained with hematoxylin and eosin (H&E) or Periodic acid–Schiff (PAS).

IgG staining of kidneys

6-µm-thick frozen sections of OCT-embedded kidneys were fixed with 3.2% formaldehyde (Polysciences, Inc.), permeabilized in 90% methanol, and incubated with blocking buffer (2% goat serum, 1% BSA, 0.1% cold fish skin gelatin, 0.1% saponin, 0.05% Tween-20 in 0.01 M PBS). Tissues were stained with Alexa-488 conjugated goat anti-mouse IgG (H+L) (Thermo Fischer). Fluorescence images were acquired using a Leica TCS SP5 II confocal microscope and Leica Acquisition Software (LAS).

Autoantibody staining of HEp-2 cells

For autoantibody staining, fixed HEp-2 antinuclear antibody (ANA) slides (MBL) were stained with diluted serum (1:50). Slides were washed and stained with either Alexa-488 conjugated goat anti-mouse IgG (H+L) or Alexa-568 conjugated goat anti-mouse IgM (Thermo Fisher) as detection antibodies. Fluorescence images were acquired using a Leica TCS SP5 II confocal microscope and Leica Acquisition Software (LAS).

Antibody quantification and ELISA

For total Ig ELISAs Immunoplate MaxiSorp plates (Thermo Fisher) were coated with 10 µg/ml goat anti-mouse IgG (heavy and light chain specific; Southern biotech) in PBS at 4°C overnight. For autoantibody ELISAs plates were coated with calf thymus dsDNA (Sigma), sm/RNP (RNA) (Sigma), or phosphatidylserine (PS) (Sigma). Plates were blocked with 1% BSA in PBS, washed then incubated with diluted sera in PBS or standards. Plates were then incubated with 1:1,000 diluted alkaline phosphatase-conjugated IgM, IgG, or IgG1 (Southern Biotech). Secondary antibodies detected by disodium p-nitrophenyl phosphate substrate (Sigma-Aldrich) and absorbance (OD) read at 405 nm.

Blood and serum glucose analysis

Blood glucose was measured via saphenous vein blood collection and levels determined with an Ascensia Contour blood glucose meter and blood glucose monitoring strips (Bayer Healthcare). Red blood cell percentages were determined by blood collection via heart puncture. Blood collected into microhematocrit tubes and spun for 120 seconds using a CritSpin Statspin centrifuge (Iris Sample Processing). Separated serum and RBC percentages were determined with a Micro Hematocrit Capillary Tube Reader (StatSpin, Iris Sample Processing).

Flow cytometry

Single cells suspensions were stained with fixable Viability Dye eFluor 780 (eBioscience) in PBS for 10 min at room temperature. Cells were stained with directly conjugated antibodies in PBS with 0.5% BCS for 20 min at 4°C. Fluorophore-conjugated antibodies purchased were from BioLegend or eBioscience. Intracellular stains were performed using a FixPerm Kit (eBioscience). To access mitochondrial membrane potential, single cell suspensions were stained for 30 minutes at 37°C in complete media with Tetramethylrhodamine, Methyl Ester, Perchlorate (TMRM, Molecular Probes). Data were acquired on an LSR II (BD Biosciences) and analyzed using FlowJo software (TreeStar).

In vitro assays

T cells were isolated from spleen and peripheral lymph nodes (LN) using CD4 or CD8 microbeads (Miltenyi). $1x10^6$ T cells were cultured with platebound α-CD3 (2C11) and α-CD28 (37.51) from BioXcell at 1μg/mL each for the indicated times. Cultures supplemented with 50U/mL (T_{conv}) or 200U/mL (T_R) IL-2 (eBioscience). Inhibitors purchased and used as follows: ZSTK474 (1μM, Sigma), Rapamycin (10nM, Selleckchem), NFAT inhibitor (10μM, Tocoris), Mek inhibitor PD0325901 (100nM, Peprotech) and Erk inhibitor FR180204 (10μM, Tocoris). *In vitro* T_R suppression assays were performed as previous described (47). Chemotaxis assay performed as previously described (48).

In vivo T_R transfer

Sorted T_R were isolated from spleen and LN as described below for Id3 T_R RNA-seq. 100,000 sorted cells were injected retro-orbitally into RAG1-deficient hosts. Spleen, LN and blood of recipient mice collected two weeks later and analyzed by flow cytometry.

CTL assay

OT-I T cells were isolated from the spleen and LN of OT-I wildtype (WT) or OT-I dLck-cre Foxo1^{CA} mice using CD8 microbeads (Miltyeni) and sorted for naïve cells based on CD8, CD44 and Foxo1^{CA}-GFP expression. Naïve T cells stimulated with platebound α-CD3 (2C11) and α-CD28 (37.51) from BioXcell at 1μg/mL for 48 hours. Cells removed from stimulation and rested overnight with fresh medium and IL-2. Target cells (APCs) isolated from congenially-marked spleen, lysed RBCs and labeled with 2.5μM cell proliferation dye (CPD) (eBioscience) at 37°C for 9 minutes and washed with FBS. CPD-labeled ACPs were pulsed with or without 10^{-7}M N4 SIINFEKL peptide for 1 hour at 37°C. APCs were washed, plated at various ratios with stimulated OT-I T cells in triplicates and incubated for 4-5 hours at 37°C. Cell cultures were stained with Live/Dead e780 (eBioscience) and run on a flow cytometer to determine viability.

VSV-OVA infections

Naïve WT OT-I and Foxo1^{CA} OT-I CD8^{+} T cells isolated and sorted as previous described for CTL assay. Cells mixed at a 1:1 ratio for a total of 10,000 T cells and injected retro-oribitally (R.O.) into congenially-marked recipient mice. One day later, recipient mice were given $1x10^{4}$ pfu of VSV-OVA in 50uL by intranasal inhalation under anesthesia. Mice were euthanized for analysis 7 days after infection. VSV-OVA provided by Dr. Pamela Fink (UW, Seattle, WA).

Diabetes induction

Naïve WT OT-I and Foxo1^{CA} OT-I CD8^{+} T cells were isolated, sorted, stimulated and rested as previously described for CTL assay. RIP.mOVA recipient mice were irradiated with 500 rad and R.O. injected with $1x10^{6}$ stimulated OT-I T cells. Mice were monitored for development of diabetes by saphenous vein blood collection and blood glucose levels determined with an Ascensia Contour blood glucose meter and blood glucose monitoring strips (Bayer

Healthcare). Mice were considered diabetic and sacrificed after two consecutive readings of glucose levels ≥300 mg/dL.

RNA-seq sample generation: Foxo1^{CA} and IRF8^{KO}

CD8^{+} T cells were isolated using CD8 microbeads (Miltenyi) from LN and spleens. For Foxo1^{CA} samples, cells were sorted from 3 individual dLck-cre^{+} Foxo1$^{CA+/-}$ Foxp3.mRFP mice and dLck-cre^{+} littermate controls. For IRF8^{KO} samples, cells were sorted from 4 individual dLck-cre^{+} IRF8$^{fl/fl}$ mice and dLck-cre^{-} IRF8$^{fl/fl}$ littermate controls. Naïve cells were sorted based on CD8, CD44, CD62L and if applicable Foxo1^{CA}-GFP expression on a FACs Aria II (BD Biosciences). Post-sort 300,000 cells were lysed with RLT buffer (Qiagen) directly for RNA or stimulated for 48 hours with platebound α-CD3 (2C11) and α-CD28 (37.51) from BioXcell at 1μg/mL and 100U/mL IL-2 (eBioscience). At 48 hours, stimulated cells were collected and lysed for RNA. RNA extracted using a TrueSeq v2 kit and libraries were constructed using the Illumina TruSeq RNA Sample Preparation kit v2. Libraries were clustered on flow cells using the TruSeq Single Read Cluster Kit v3, followed by single-read sequencing for 50 cycles on a HiSeq2500 sequencer (Illumina, CA).

RNA-seq sample generation: Id3 T_R

CD4^{+} T cells were isolated using CD4 microbeads (Miltenyi) from either peripheral LNs or spleens of 3 littermate Id3-GFP x Foxp3-mRFP mice. Cells were sorted based on viability, CD4, CD44, CD62L, Id3-GFP and Foxp3-mRFP expression on a FACs Aria II (BD Biosciences). 500 cells were sorted directly into SMART-Seq v4 Ultra Low Input RNA Kit (Takara) lysis buffer and cDNA produced by following the kit protocol. Library construction was performed using a modified protocol of the NexteraXT DNA sample preparation kit (Illumina).

RNA-seq analysis

Dual-index, single-read sequencing of pooled libraries was run on a HiSeq2500 sequencer (Illumina) with 58-base reads and an average depth of 8.6Mio reads per library (for Id3), 13.5 Mio reads per library (for those libraries that passed QC in Foxo1^{CA}) and 16 Mio reads per library (for IRF8). Base-calling and demultiplexing were performed automatically on BaseSpace (Illumina) to generate FASTQ files.

FASTQ files were processed to remove reads of zero length (fastq_trimmer v.1.0.0), remove adapter sequences (fastqmcf tool v.1.1.2) and perform quality trimming from both ends until a minimum base quality ≥ 30 (FASTQ quality trimmer tool v.1.0.0). Reads were aligned to the mouse reference genome (build NCBI37) with TopHat (v.1.4.0) and read counts per Ensembl gene ID were quantified with htseq-count (v.0.4.1). Quality metrics for the FASTQ and BAM/SAM files were generated with FastQC (v.0.11.3) and Picard (v.1.128). Processing of FASTQ and BAM/SAM files was executed on the Galaxy workflow platform of Globus genomics.

Statistical analysis of gene expression was assessed in the R environment (v.3.4.4). All samples with > 90% of reads mapping to the reference genome and median CV coverage < 0.55 went into downstream processing. One sample (naïve Ctrl from Foxo1 experiment) didn't pass QC and was excluded. We mapped Ensembl Gene IDs to MGI gene symbols using biomaRt (v2.32.2) and filtered out lowly expressed transcripts and non-protein coding genes. In order to normalize counts between samples, we computed scaling factors for the raw library sizes with edgeR::calcNormFactors (v.3.20.9). We normalized libraries and assessed their differential gene expression separately for each of the 3 experiments. A linear model was fit to each gene with limma (v.3.34.9), making pairwise comparisons between the populations of interest as contrasts. Differentially expressed genes were defined as adj.p.value < 0.05 and log2FC > 1 (for Id3 and Foxo1^{CA}) and adj.p.value < 0.05 without additional logFC cutoff (for IRF8). The log expression values were z-transformed by row in all heatmaps and the column dendrograms on top of the plots represents hierarchical clustering of Euclidean distances.

Functional enrichment was assessed by taking the geneset of DE genes and running goseq (v.1.30.0) to determine enrichment of gene ontology (GO) categories. Results were filtered for categories with a size < 500 (for Id3), and size < 400 (for Foxo1). Barcode plots for enrichment of gene signatures were generated with limma::barcodeplot and significance determined by rotation gene set tests with limma::roast.

Statistical analysis

The p values were calculated by Prism software (GraphPad) using either an unpaired Student's t test or one-way ANOVA as indicated. Values less than 0.05 were considered significant.

Chapter 3:

T cell-specific constitutive activation of Foxo1 results in spontaneous inflammatory disease

Introduction

The Foxo (forkhead box O) family of transcription factors are important for maintaining homeostasis of a variety of cell types throughout the body. This family of transcription factors regulate the genome by binding DNA through their conserved forkhead domain, allowing for either activation or suppression of target genes. Members of this family have diverse roles in regulating cell homeostasis, metabolism, cell cycle, DNA repair and apoptosis (41, 49). Foxo family members have been extensively studied as tumor suppressors due to their role in regulating cell cycle checkpoints (50, 51). Additionally Foxo family members can sense and respond to oxidative stress, insulin and growth factors.

Of the four family members, Foxo1 and Foxo3 are the most highly expressed in the immune system, with naïve T and B cells expressing high levels of Foxo1 (36, 41, 52-54). In B and T cells, Foxo1 is phosphorylated downstream of the PI3K/Akt/mTOR signaling pathway, through BCR and TCR signaling respectively, resulting in its inactivation and translocation from the nucleus and subsequent altered transcription of downstream targets. Alternatively, Foxo1 can be inactived by acetylation, although a role for this mechanism has not been demonstrated in T or B cells (55).

In B cells Foxo1 is the predominate Foxo family member expressed during development, with high expression starting at pro-B stage (54). Foxo1 regulates B cell maturation through promotion of several key genes. Foxo1 but not Foxo3, promotes expression of *Rag1* and *Rag2*, aiding in successful V(D)J rearrangement (56). Additionally deletion of Foxo1 at the pro-B stages of development resulted in apoptosis of immature B cells due to a lack of IL-7R

expression and downstream survival signals. In both B and T cells, active Foxo1 binds to the IL-7Rα gene, promoting expression of the IL-7R (52). In germinal center (GC) B cells, Foxo1 controls cycling between the light and dark zone, with high Foxo1 expression in the dark zone and PI3K mediated downregulation of Foxo1 promoting migration to the light zone (57).

Mice lacking Foxo1 in T cells have an overall reduced T cell compartment, reduced naïve T cells and increased frequencies of effector T cells (44, 53, 58). These studies again identified *Il7rα* gene as a target of Foxo1 binding, with active Foxo1 binding to and promoting expression of IL-7Rα. Along with the common γ chain, IL-7Rα signaling is important in promoting T cells proliferation and survival. Additionally Foxo1 binds to and regulates *Klf2,* which controls expression of L-selectin (CD62L) and S1PR1, receptors which control naïve T cell migration and retention in lymphoid organs (53, 59, 60). More recent work has identified Foxo1 as an important competitor and advocate of Foxp3, regulating both T_R development and function. In T_R Foxo1 and Foxp3 have overlapping binding DNA sites in select regions of the genome, where bound Foxo1 helps maintain an established enhancer region which Foxp3 can bind to (61, 62). In this model TCR stimulation phosphorylates Foxo1, thus promoting its inactivation and translocation from the nucleus. At the same time, stimulation upregulates Foxp3 which can now bind to enhancer regions previously occupied by Foxo1. As such, sustained occupancy by Foxo1 can hinder binding by Foxp3, allowing for competition and fine tuning of genomic landscapes at specific DNA sites. Together these data highlight the importance of Foxo1 regulation and specifically its inactivation.

While many studies have examined the effects of Foxo1 deficiency, few have examined the processes affected by downregulation of Foxo1 rather than its absence. Thus, we asked how does sustained activation of Foxo1 affect T cell homeostasis and function? To address this question we obtained mice expressing a non-phosphorylatable version of Foxo1 knocked into the ROSA26 locus with a ‘stop-flox’ cassette. Using two different transgenic cre mice allowed us

to examine the effects of sustained Foxo1 expression specifically in T cells either during or post thymic development.

Results

CD4cre Foxo1^{CA} mice develop spontaneous inflammatory disease

To examine regulation of Foxo1, we obtained mice with a human version of the Foxo1 gene in which the 3 Akt-targeted phosphorylation sites, Thr-24, Ser-256, and Ser-319, have been mutated to alanine residues (Foxo1^{CA}). This modified Foxo1 gene was knocked in to the ubiquitously-expressed ROSA26 locus, along with a 'stop-flox' cassette that prevents expression (29, 44). We generated CD4-cre x Foxo1^{CA} reporter mice, in which Foxo1 is constitutively active in all CD4^{+} and CD8^{+} T cells starting the CD4^{+} CD8^{+} double positive phase of thymic development. For all studies we examined mice with one copy of the CD4-cre transgene and one copy of the Foxo1^{CA} allele, referred to as CD4cre Foxo1^{CA} mice. We observed that CD4cre Foxo1^{CA} mice were runted compared to littermate controls starting around 5 weeks of age (Fig 3.1A) and had splenomegaly but not lymphadenopathy (Fig 3.1B). General appearance and body condition of CD4cre Foxo1^{CA} mice continued to deteriorate over time, with development of dermatitis (Fig 1C), hypoglycemia and anemia (Fig 3.1D-E). Histology revealed inflammation and increased cell infiltrated in the skin and lung, along with increased mucus production in CD4cre Foxo1^{CA} mice compared to littermate controls (Fig 3.1C).

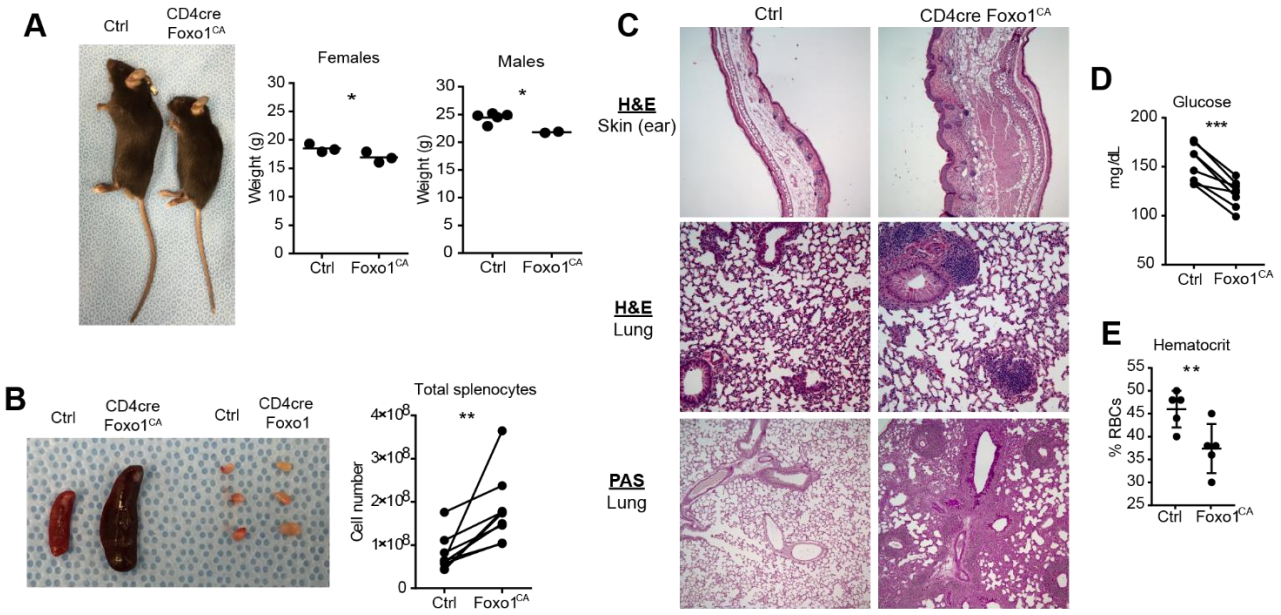

Figure 3.1: CD4cre Foxo1^{CA} mice develop spontaneous inflammatory disease

A) Left: Representative pictures of runting and reduced body weight observed in 9 week old CD4cre Foxo1^{CA} mice and littermate controls. Right: Graphed weights B) Left: Representative pictures of splenomegaly but not lymphadenopathy. Right: Absolute cell number of the spleen. C) H&E or PAS staining of skin and lung tissue from 10-12 week old CD4cre Foxo1^{CA} mice and littermate control tissue at 10x magnification. D) Blood glucose levels measured by saphenous vein bleeding of 12 week old CD4cre Foxo1^{CA} mice and littermate controls. E) Percent red blood cells in collected blood of 12 week old mice. Significance determined by paired students t-test, *p <0.05, **p < 0.01, ***p < 0.001.

CD4cre Foxo1^{CA} mice have reduced peripheral T cell numbers

In both the spleen and LN of CD4cre Foxo1^{CA} mice, we observed an altered T cell compartment. CD4cre Foxo1^{CA} mice had decreased CD4^{+} T cells with similar numbers of CD8^{+} T cells (Fig 3.2A). Architecture of CD4cre Foxo1^{CA} spleens were disrupted with no discernable T cell zone and more dispersed B cell zones (Fig 3.2B). Both CD4^{+} and CD8^{+} T cells in CD4cre Foxo1^{CA} mice were skewed towards an activated phenotype with high CD44 expression in spleen and LN (Fig 3.2C). T cells also produced increased pro-inflammatory cytokines, IL-4 and INFɣ upon ex vivo stimulation with PMA, ionomycin and monensin (Fig 3.2D). Interestingly adult CD4cre Foxo1^{CA} mice had thymic remnants (not shown), suggesting either inflammation-mediated destruction of the thymus or decreased thymic output. To test if decreased CD4^{+} T cell numbers were due to inflammation or altered thymic maturation we examined neonatal CD4cre Foxo1^{CA} mice. Of note neonatal CD4cre Foxo1^{CA} mice appeared healthy, with similar body and spleen weights as littermate controls (data not shown). Total thymocyte cell number were similar between CD4cre Foxo1^{CA} and littermate control mice from 2 to 9 days old (Fig 3.2E). However at 12 days old we noted a decrease in total cells and double positive thymocytes (Fig 3.2E). Interestingly we noted decreased maturation of single positive CD4^{+} T cells at all examined ages in the thymus but no significant differences in single positive CD8^{+} T cells (Fig 3.2E). Together these data suggest that the reduced CD4^{+} T cells observed in the periphery of adult mice is due to a reduction of single positive CD4^{+} T cell maturation in the thymus due to expression of the Foxo1^{CA} allele.

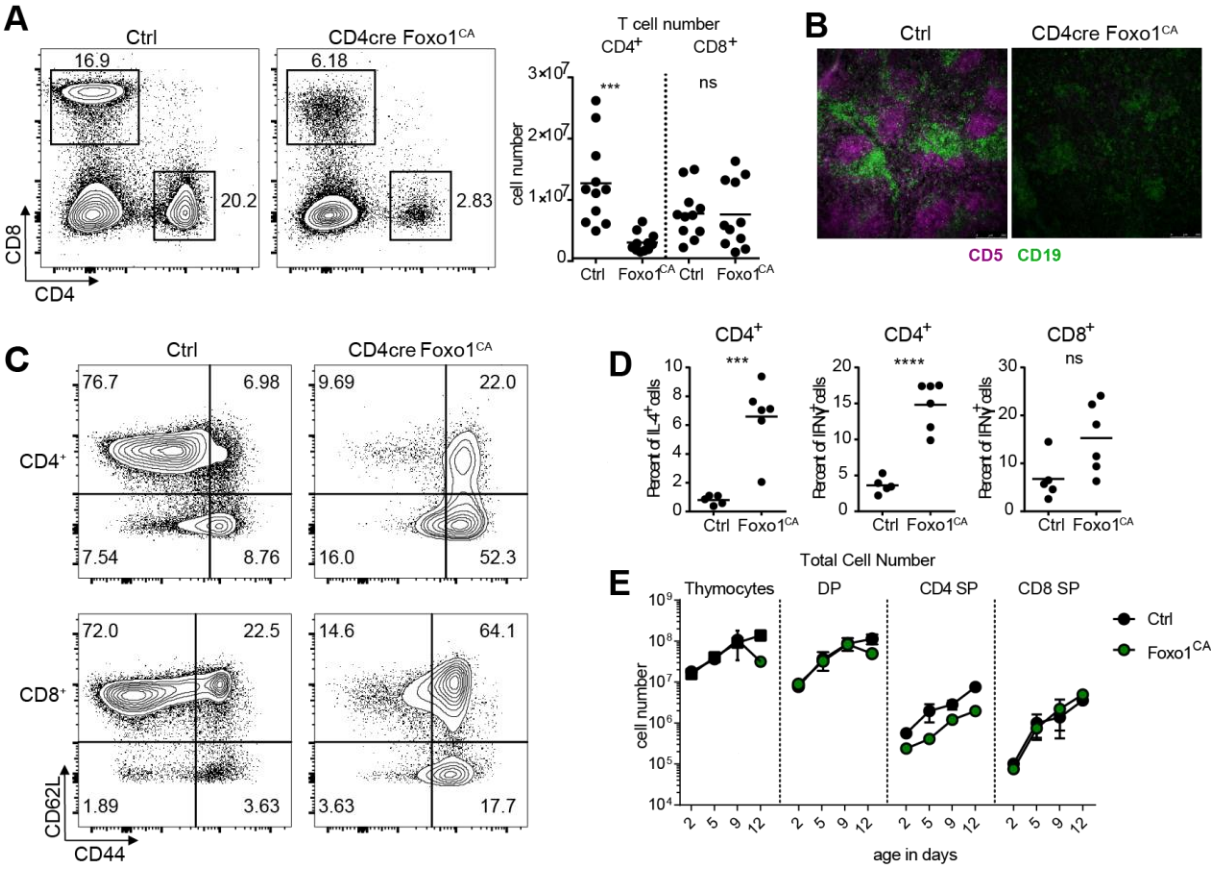

Figure 3.2: CD4cre Foxo1^{CA} mice have reduced peripheral T cell numbers

a) Representative flow cytometry plots and graphical analysis of splenic CD4 and CD8 T cells gated on live lymphocytes. B) Representative microscopy staining of B and T cell zones in the spleen C) Representative flow cytometry plots of CD44 and CD62L expression by gated splenic TCRβ^{+} CD4^{+} or CD8^{+} T cells. D) Graphical analysis of cytokine production by PMA/ionomycin with monensin (4 hrs) stimulated splenic and LN T cells. E) Frequency and absolute number of thymocytes recovered from 2-12 day old CD4cre Foxo1^{CA} mice. DP are CD4^{+} CD8^{+} double positive cells and SP are single positive cells for indicated CD4 or CD8. Significance determined by unpaired students t-test, *p <0.05, **p < 0.01, ***p < 0.001, ****p < 0.0001.

CD4cre Foxo1^{CA} mice have reduced T_R but this is not the sole cause of inflammation

Corresponding with decreased CD4$^+$ T cells we observed reduced frequency and numbers of T_R in CD4cre Foxo1^{CA} mice (Fig 3.3A). Thus we hypothesized that inflammation in CD4cre Foxo1^{CA} mice was due to a lack of regulation by T_R. As such we performed neonatal T_R rescues to restore regulation of effector T cells. We transferred WT T_R intraperitoneally into neonatal CD4cre Foxo1^{CA} mice at 5 days old and monitored for 12 weeks. Transfer of WT T_R into CD4cre Foxo1^{CA} mice improved overall body condition and weight but did not prevent inflammation (data not shown and Fig 3.3B). WT T_R recipient CD4cre Foxo1^{CA} and un-injected littermate CD4cre Foxo1^{CA} mice had comparable splenomegaly, reduced CD4$^+$ T cells and activation of effector T cells (Fig 3.3C-D). Additionally antibody depletion of CD8$^+$ T cells did not reduce dermatitis or splenomegaly or restore body weight (data not shown). Together these data suggest that inflammation in CD4cre Foxo1^{CA} mice is not rescued by T_R-mediated suppression.

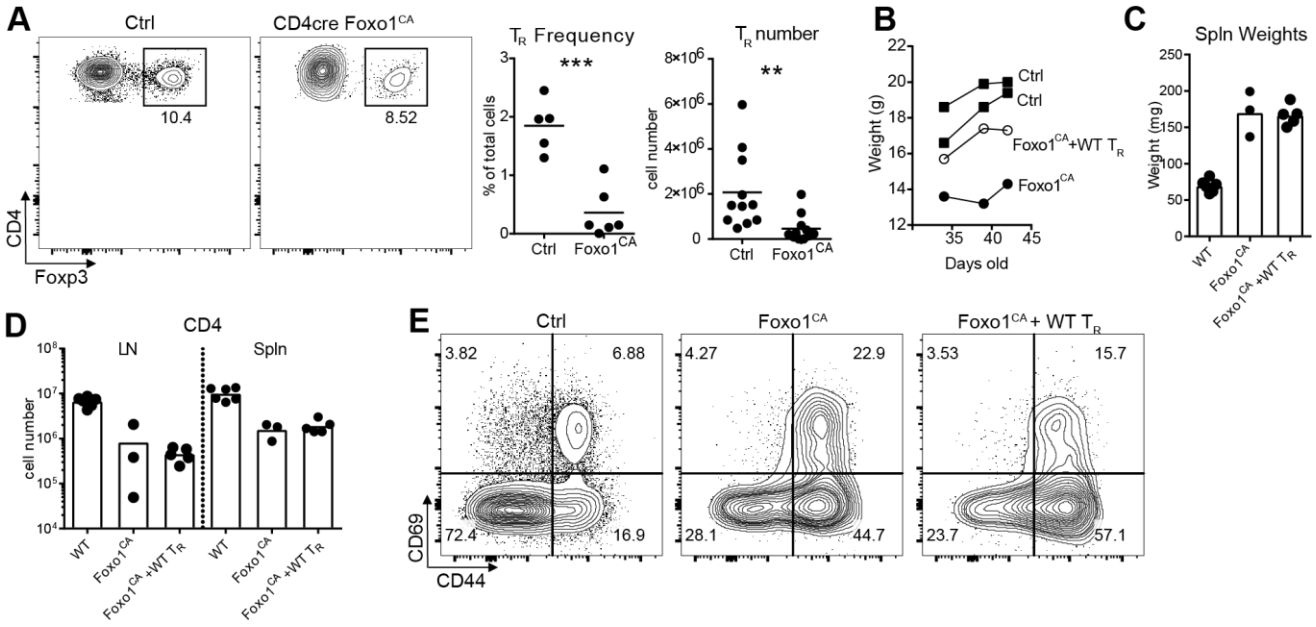

Figure 3.3: CD4cre Foxo1^{CA} mice have reduced T_R but inflammation is not solely due to lack of T_R

A) Representative flow cytometry plots and graphical analysis of Foxp3 expressing T_R within gated splenic TCRβ$^+$ CD4$^+$ T cells of 12 week old CD4cre Foxo1^{CA} mice and littermate controls. B-C) Representative body weights of CD4cre Foxo1^{CA} mice injected IP with WT T_R at 5 days old and uninjected littermate controls. C) Spleen weight of of CD4cre Foxo1^{CA} mice injected IP with WT T_R at 5 days old and uninjected littermate controls. Pooled from 3 independent experiments D) Cell number of CD4$^+$ T cells in the LN or spleen of of CD4cre Foxo1^{CA} mice injected IP with WT T_R at 5 days old and uninjected littermate controls. Pooled from 3 independent experiments. E) Representative flow cytometry plots of gated splenic CD4$^+$ T cells from of CD4cre Foxo1^{CA} mice injected IP with WT T_R at 5 days old and uninjected littermate controls at 9 weeks of age. Significance determined by unpaired students t-test, **p < 0.01, ***p < 0.001.

Altered B cell compartment in CD4cre Foxo1^{CA} mice results in class switched and autoantibody production

Examining the splenomegaly in CD4cre Foxo1^{CA} mice, it is clear that B cells were the most significantly expanded lymphocyte population (Fig 3.4A) with similar numbers of dendritic cells and moderate increases in monocytes and neutrophils (data not shown). CD4cre Foxo1^{CA} mice had increased frequency and number of total B cells in peripheral LNs and spleen compared to controls. CD4cre Foxo1^{CA} mice had an increase of GC B cells in LNs but not spleens, most likely due to disrupted splenic architecture inhibiting defined T:B zone formation (Fig 3.2B). Serum ELISAs revealed an increase in total IgG in CD4cre Foxo1^{CA} mice compared to controls (Fig 3.4C). Isotype-specific ELISAs showed a decrease in circulating IgA and IgG2b, antibodies known to promote protection at barrier sites (Fig 3.4C) (63, 64). Conversely, CD4cre Foxo1^{CA} mice had increased levels of IgM and IgG1 (Fig 3.4C). We stained HEp-2 cells to determine staining patterns and potential auto-antigens these antibodies targeted. Total Ig H+L staining revealed unique staining of cytoplasm, compared to the normally observed nuclear staining in lupus models (65, 66). Further staining with select antibody isotypes revealed all auto-antibody staining was IgM-mediated (Fig 3.4D). We confirmed these results by performing isotype-specific ELISAs against RNA, DNA and phosphoryl serine and again observed that only IgM antibodies were auto-reactive in CD4cre Foxo1^{CA} mice (Fig 3.4E). In addition to increases in total serum antibodies, we noted antibody deposits in the kidneys of CD4cre Foxo1^{CA} mice, commonly known as glomerulonephritis, a condition normally seen in lupus (Fig 3.4F) (66). Together these data demonstrate that a majority of the inflammation observed in CD4cre Foxo1^{CA} mice is driven by autoreactive B cell responses.

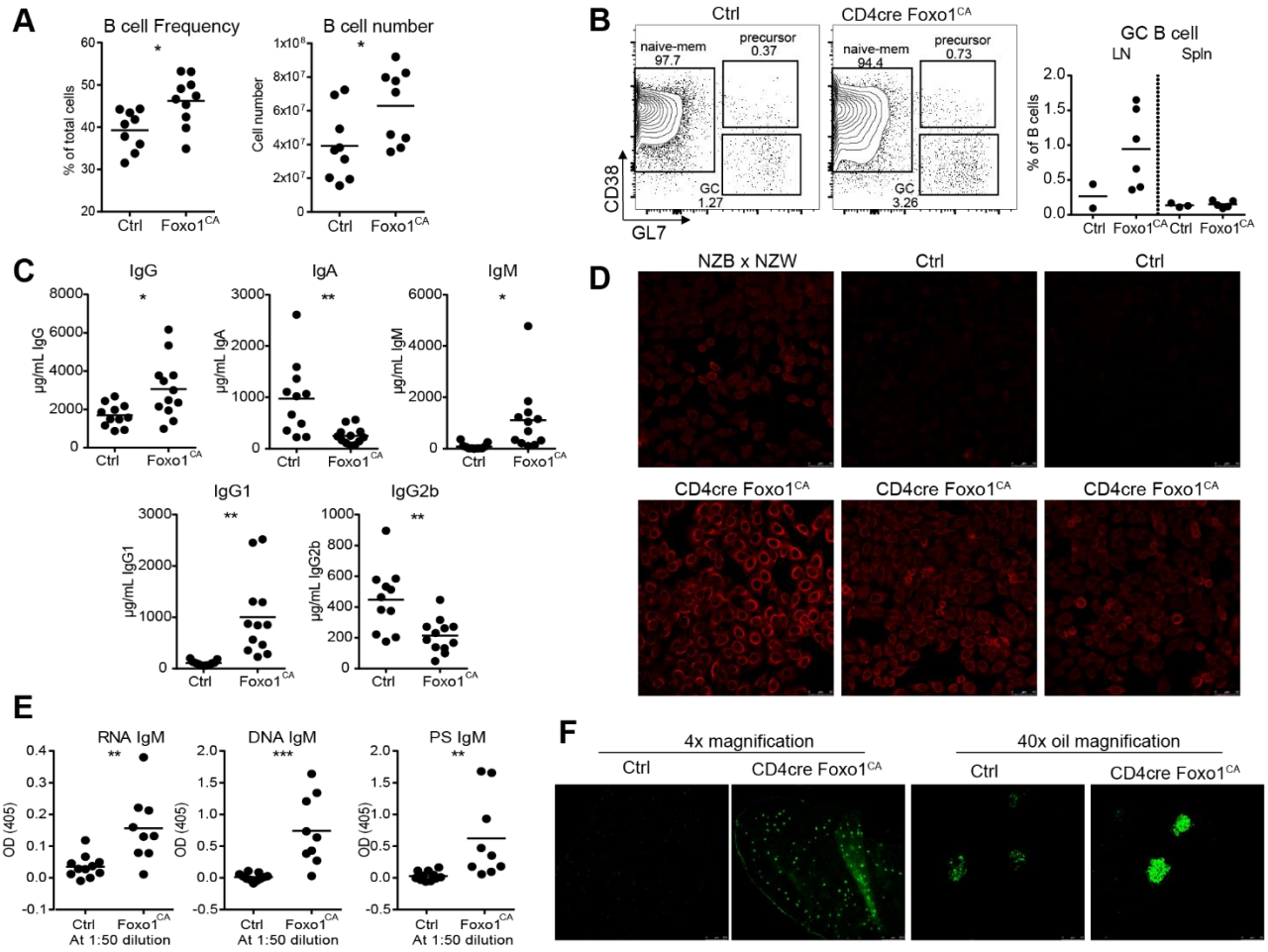

Figure 3.4: Altered B cell compartment in CD4cre Foxo1^{CA} mice results in class switched and auto-antibody production.

A) Frequency and cell number of B cells in the spleen of CD4cre Foxo1^{CA} mice and littermates. B) Representative flow cytometry plots and graphical analysis of LN GC B cells gated on CD19^{+}, GL-7 and CD38 staining. C) Serum antibody levels measured by ELISA in 6-12 week old mice. Data from >4 independent experiments. D) Top: Representative microscopy staining of HEp-2 ANA slides. Stain with serum diluted 1:50 and anti-IgM specific secondary. E) Serum IgM auto-reactive antibodies measured by ELISA. F) Representative microscopy staining of frozen kidney sections. Stained for total Ig (anti-mouse IgG H+L). Significance determined by unpaired students t-test, *p <0.05, **p < 0.01, ***p < 0.001.

Discussion

This work highlights a previously under appreciated mechanism by which Foxo1 expression is regulated during thymic development. Although complicated to study and not fully understood, PI3K signaling is essential for proper thymic development. Several groups have demonstrated that inhibition of PI3K-Akt signaling or deficiencies in PI3K subunits result in decreased double positive and mature T cells (67). These data suggest that the PI3K cascade is active in the thymus and might promote inactivation of Foxo1 during thymic development. In CD4cre Foxo1^{CA} mice, the Foxo1^{CA} allele is turned on at the double positive phase of thymic development due to expression of CD4 and subsequent cre-mediated recombination. Normally thymocytes have low or undetectable levels of Foxo1 until positive selection and commitment to either the CD4 or CD8 lineage (50). Active Foxo1 promotes expression of the chemokine receptor CCR7, which regulates thymocyte maturation through their directed migration between the cortex and medulla by following CCR7 ligand gradients (53, 68, 69). Thus we hypothesize that Foxo1 expression and activation is tightly regulated through PI3K signaling in the thymus to prevent aberrant migration of developing thymocytes. We propose that in CD4cre Foxo1^{CA} mice, CCR7 is expressed at the double positive phase instead of later, during positive selection, leading to early migration of thymocytes and failure to proceed past positive selection. In agreement with this hypothesis, expression of CCR7 prior to positive selection leads to mislocalization of thymocytes and decreases in mature single positive CD4$^+$ T cells (69). Interestingly, single positive CD8$^+$ T cells are more reliant on CCR7 signaling for maturation (70), giving a possible explanation for the normal numbers and frequencies of CD8$^+$ T cells observed in CD4cre Foxo1^{CA} mice. These data highlight the importance of regulating Foxo1 expression during thymic development and suggest that dysregulation can lead to reduced mature T cells and inflammation.

In the periphery we noted reduced $CD4^+$ T cells, corresponding with decreased thymic output. Both $CD4^+$ and $CD8^+$ T cells were highly activated and made inflammatory cytokines, likely contributing to chronic inflammation observed in CD4cre $Foxo1^{CA}$ mice. These results have been confirmed by collaborators who also observed inflammatory disease in CD4cre $Foxo1^{CA}$ mice in a different facility, highlighting the T cell intrinsic nature of this disease (71). To test if inflammation was T cell intrinsic, Newton *et al.* made mixed bone marrow chimeras with WT and CD4cre $Foxo1^{CA}$ bone marrow. Chimeric mice were healthy, with the majority of $CD4^+$ T cells and T_R derived from WT bone marrow, suggesting restored tolerance from WT T cells. Intriguingly the $CD8^+$ T cell compartment was equally made up of WT and $Foxo1^{CA}$ derived T cells, suggesting different mechanisms of Foxo1 regulation between CD4 and CD8 T cells during thymic development as we hypothesized.

The data in this chapter describe spontaneous autoimmune disease observed in CD4cre $Foxo1^{CA}$ mice due to unchecked B cell responses mediated by dysregulation of Foxo1 during thymic development. One outstanding question is, what initiates B cell driven autoimmunity in CD4cre $Foxo1^{CA}$ mice? Mice with mutations in the TCRα gene, which lack mature single positive T cells, develop gut inflammation but not until 4-5 months of age (72). This is in contrast to CD4cre $Foxo1^{CA}$ mice which show signs of inflammation as early as 5 weeks old. It remains to be determined if CD4cre $Foxo1^{CA}$ mice have increased apoptosis, altered mucosal barriers or other defects which can lead to early development of inflammation. Future studies are required to determine the exact mechanisms driving the onset of autoimmunity in CD4cre $Foxo1^{CA}$ mice.

Chapter 4:

Foxo1 inactivation is essential for $CD8^+$ effector T cell function

Introduction

Despite its known role in regulating effector T cell differentiation and function, the precise mechanisms by which Foxo1 regulates $\alpha\beta$ T cells are still being determined. Downregulation of Foxo1 is a dynamic process in which active Foxo1 is bound to DNA in the nucleus, and upon TCR stimulation, Foxo1 is phosphorylated by PI3K-Akt, resulting in its inactivation and exit from the nucleus (73, 74). Discontinuing TCR stimulation, T cells will regain active Foxo1 and varied expression of Foxo1 regulates cell fates between long and short lived effector-memory $CD8^+$ T cells (75, 76). While many studies have examined the importance of active or total Foxo1, few have addressed the temporal dynamics of Foxo1 inactivation. Foxo1's role in maintaining the naïve T cell pool through CD62L, IL-7Rα and CCR7 expression is well documented, with mice lacking Foxo1 having reduced naïve T cell pools and increased effector frequencies (53, 60). Recently new tools have allowed for more nuanced examination of Foxo1 regulation with deletion of Foxo1 at select timepoints initiated by treating ER-cre Foxo1-floxed mice with tamoxifen. Delpoux *et al.* found that during infection, Foxo1 controls the $CD8^+$ T cell switch between memory-effector and short-lived effectors (77). Deletion and thus inactivation of Foxo1 prior to infection resulted in short-lived apoptotic-prone effector $CD8^+$ T cells. Together these data demonstrate that Foxo1 activation and subsequent inactivation is a dynamic process, continuously fine-tuned during the lifetime of a T cell. As such, we sought to examine the initial inactivation of Foxo1 in naïve T cells during primary stimulation.

In the previous chapter, we examined how sustained activation of Foxo1 during thymic development altered T cell homeostasis and function. Active Foxo1 expression in double

positive thymocytes resulted in reduced $CD4^+$ T cells and spontaneous autoimmune disease starting around weaning. Due to this early onset of inflammation we were unable to answer our original research question, how does sustained activation of Foxo1 affect T cell homeostasis and function? To re-address this question, we utilized a different transgenic cre model, distal-Lck-cre, to induce sustained expression of Foxo1 after thymic maturation. Mice with the $Foxo1^{CA}$ allele turned on after thymic egress were healthy with normal numbers of T cells, allowing us to better interrogate the role of Foxo1 in regulating mature T cell function.

Results

Sustained expression of Foxo1 inhibits effector and T_R cell generation

To examine the role of Foxo1 inactivation in the absence of inflammation, we utilized distal-Lck-cre mice, in which cre-recombinase turns on post-thymic selection. We generated dLck-cre^+ $Foxo1^{CA+/-}$ mice, which had one copy of the dLck-cre transgene and one copy of the $Foxo1^{CA}$ allele, herein referred to dLck-cre $Foxo1^{CA}$. Unlike CD4cre $Foxo1^{CA}$ mice, dLck-cre $Foxo1^{CA}$ mice were healthy, with normal weight, lymphocyte number and serum antibody levels (data not shown). In the $CD4^+$ T cell compartments, we observed partial recombination of the ROSA26-$Foxo1^{CA}$ allele with 40-50% of $CD4^+$ T cells expressing GFP and thus the constitutively active Foxo1 allele ($Foxo1^{CA}$) (Fig 4.1A). Gating $CD4^+$ T cells based on GFP expression, almost all $CD44^{hi}$ effector T cells and T_R found in dLck-cre $Foxo1^{CA}$ mice were GFP^- (Fig 4.1A), suggesting that inactivation of Foxo1 is essential for both effector T cell and T_R formation. Indeed, through knockout studies, others have reported on the importance of proper Foxo1 regulation for the maintenance and function of these subsets (29, 44). Striking in the $CD8^+$ T cell compartment there was more cre-mediated recombination with 80-90% of T cells being GFP^+ (Fig 4.1A). As in the $CD4^+$ T cell compartment, we observed a skewing of GFP^+ ($Foxo1^{CA}$) T cells towards a naïve phenotype, with the majority of central memory and effector T cells falling in the GFP^-

compartment. For a control we obtained Ai6 transgenic mice, which have the ROSA26-GFP allele but do not contain a gene of interest (45). When examining dLck-cre Ai6 mice, we noted almost all T cells had recombined, expressing GFP equally in both the $CD4^+$ and $CD8^+$ T cell compartments (Fig 4.1C-D). Of particular note, GFP^+ T cells contained normal frequencies of naïve T cells, effector T cells and T_R (Fig 4.1C-D). Together these data demonstrate that sustained activation of Foxo1 prevents both T_R and effector T cell generation *in vivo*.

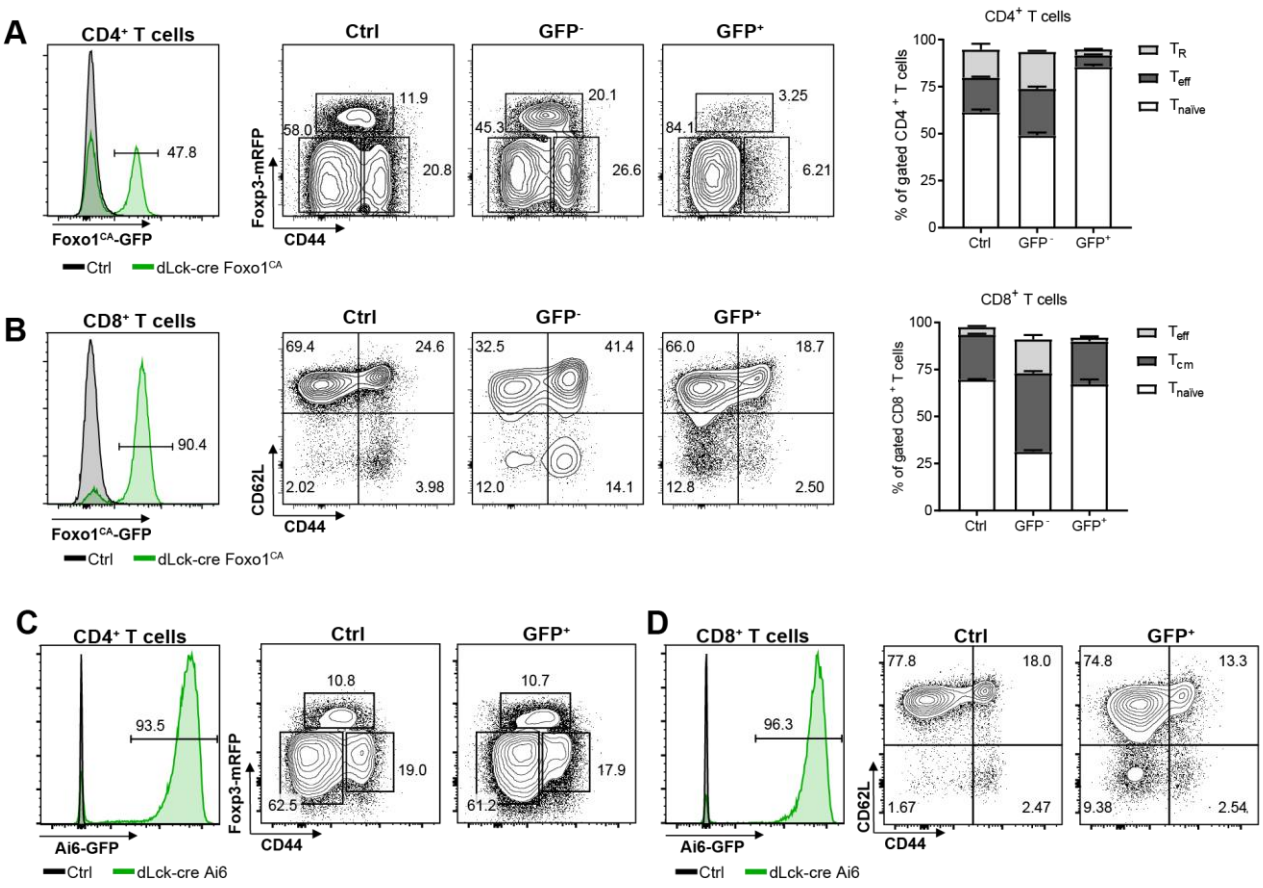

Figure 4.1: Sustained expression of Foxo1 inhibits effector and T_R cell generation

A) (Left) Representative histograms of Foxo1^{CA}-GFP expression by gated splenic TCRβ$^+$ CD4$^+$ T cells. Representative flow cytometry plots of Foxp3-mRFP and CD44 expression on gated control, GFP$^-$ (Foxo1^{CA-}) and GFP$^+$ (Foxo1^{CA+}) TCRβ$^+$ CD4$^+$ T cells. (Right) Graphical analysis of the indicated populations. B) (Left) Representative histograms of Foxo1^{CA}-GFP expression by gated splenic TCRβ$^+$ CD8$^+$ T cells. Representative flow cytometry plots of CD62L and CD44 expression on gated control, GFP$^-$ (Foxo1^{CA-}) and GFP$^+$ (Foxo1^{CA+}) TCRβ$^+$ CD8$^+$ T cells. (Right) Graphical analysis of indicated populations. C) Representative histograms of Ai6-GFP expression and flow cytometry plots of Foxp3-mRFP and CD44 expression on gated splenic TCRβ$^+$ CD4$^+$ T cells. D) Representative histograms of Ai6-GFP expression and flow cytometry plots of CD62L and CD44 expression on gated splenic TCRβ$^+$ CD8$^+$ T cells. All data from 10 week old reporter mice and littermate controls.

Sustained expression of Foxo1 inhibits effector T cell function

To test if naïve Foxo1^{CA} CD8^{+} T cells were capable of activation and differentiation into effectors, we first utilized *in vitro* cultures. We sorted naïve CD8^{+} T cells from peripheral LN and spleens of dLck-cre Foxo1^{CA} mice and littermate controls. Cells were stimulated for 48 hours with platebound αCD3/28 and supplemented with IL-2, and analyzed by flow cytometry. Stimulated Foxo1^{CA} cells upregulated CD44 and CD69 to similar levels as control cells (Fig 4.2A), suggesting that these cells can be activated. However Foxo1^{CA} cells maintained high CD62L expression, likely due to continued positive regulation of CD62L expression through Foxo1/Klf2 binding to the promoter of *Sell* (CD62L) (53). Furthermore, at these early time points of activation, Foxo1^{CA} and control cells proliferated to a similar degree (Fig 2B). To test mitochondrial function we stained naïve and stimulated cells with tetramethylrhodamine, methyl ester, perchlorate (TMRM), a dye which is sequestered by active mitochondria. Although not a direct measure of OXPHOS, TMRM staining can show relative mitochondrial activity, with high TMRM staining indicating active mitochondria (OXPHOS) and lower TMRM staining suggesting less active mitochondria (glycolysis) (78, 79). In line with their proliferation and expression of activation markers, stimulated Foxo1^{CA} T cells had reduced TMRM uptake compared to naïve cells, indicating metabolic switching after stimulation. Of interest, stimulated Foxo1^{CA} T cells had slightly higher levels of TMRM than stimulated control cells, maybe hinting at defects in metabolism (Fig 4.2C). Given its known role in regulating metabolism, future studies could examine regulation of metabolism by Foxo1 in effector T cells (80). Additionally, stimulated Foxo1^{CA} T cells failed to make the traditional effector CD8^{+} T cell cytokines, granzyme B, IFNɣ and TNFα (Fig 4.2D). Together these data suggest that Foxo1^{CA} cells activate but do not fully transition to effector cells. In agreement with this, *in vitro* CTL killing assays demonstrated that Foxo1^{CA} OT-I cells failed to kill target cells as well as control OT-I cells (Fig 4.2E).

To examine activation and effector function *in vivo* we transferred OT-I T cells into naïve mice and induced a model of autoimmunity or infection. First, to examine primary stimulation *in* vivo, we transferred a 1:1 ratio of sorted naïve wildtype (WT) OT-I and Foxo1^{CA} OT-I T cells retro-orbitally into congenic recipient mice. Mice were intranasally infected with VSV-OVA and analyzed 7 days later for expansion of transferred antigen-specific CD8^{+} T cells (81). At the primary site of infection, the lung, over 80% of recovered transferred cells were WT OT-I T cells (Fig 4.2F). In lung, spleen and mediastinal LNs, WT and Foxo1^{CA} OT-I T cells were activated, with high expression of CD44 (not shown), although Foxo1^{CA} T cells still maintained high CD62L expression as observed previously in *in vitro* stimulations (Fig 4.2A). Interestingly more Foxo1^{CA} OT-I cells than WT OT-I were recovered from mediastinal LNs, suggesting that in addition to reduced effector function, Foxo1^{CA} T cells may have impaired migration to inflamed tissues (Fig 4.2F). Indeed, active Foxo1 promotes expression of CCR7 and CD62L which helps retain lymphocytes in secondary lymphoid organs (53). Second, we turned to a model of autoimmunity in which diabetes is induced by transferring stimulated OVA specific CD8^{+} T cells (OT-I) into mice expressing a membrane-bound form of OVA under control of the rat insulin promoter (RIP-mOVA) which drives OVA expression primarily in β islets in the pancreas (82). In this model primary *in vitro* stimulation is antigen independent, with secondary stimulation both antigen and tissue specific (83). We stimulated sorted naïve WT or Foxo1^{CA} OT-I T cells *in vitro* with platebound αCD3/CD28 for 48 hours and then the cells were rested overnight. Activated cells were transferred retro-orbitally into sublethatlly-irradiated RIP-mOVA mice to induce diabetes. WT OT-I recipient mice developed diabetes 5 days after transfer but Foxo1^{CA} OT-I recipients remained healthy (Fig 4.2G). These data suggest that addition of a secondary stimulation does not overcome effector cell defects observed in Foxo1^{CA} T cells. Together these two *in vivo* models demonstrate that sustained activation of Foxo1 inhibits effector T cell function. However it remains to be determined if defective effector function of Foxo1^{CA} cells is limited to failure to make cytokines and/or defects in proliferation and survival at these later timepoints.

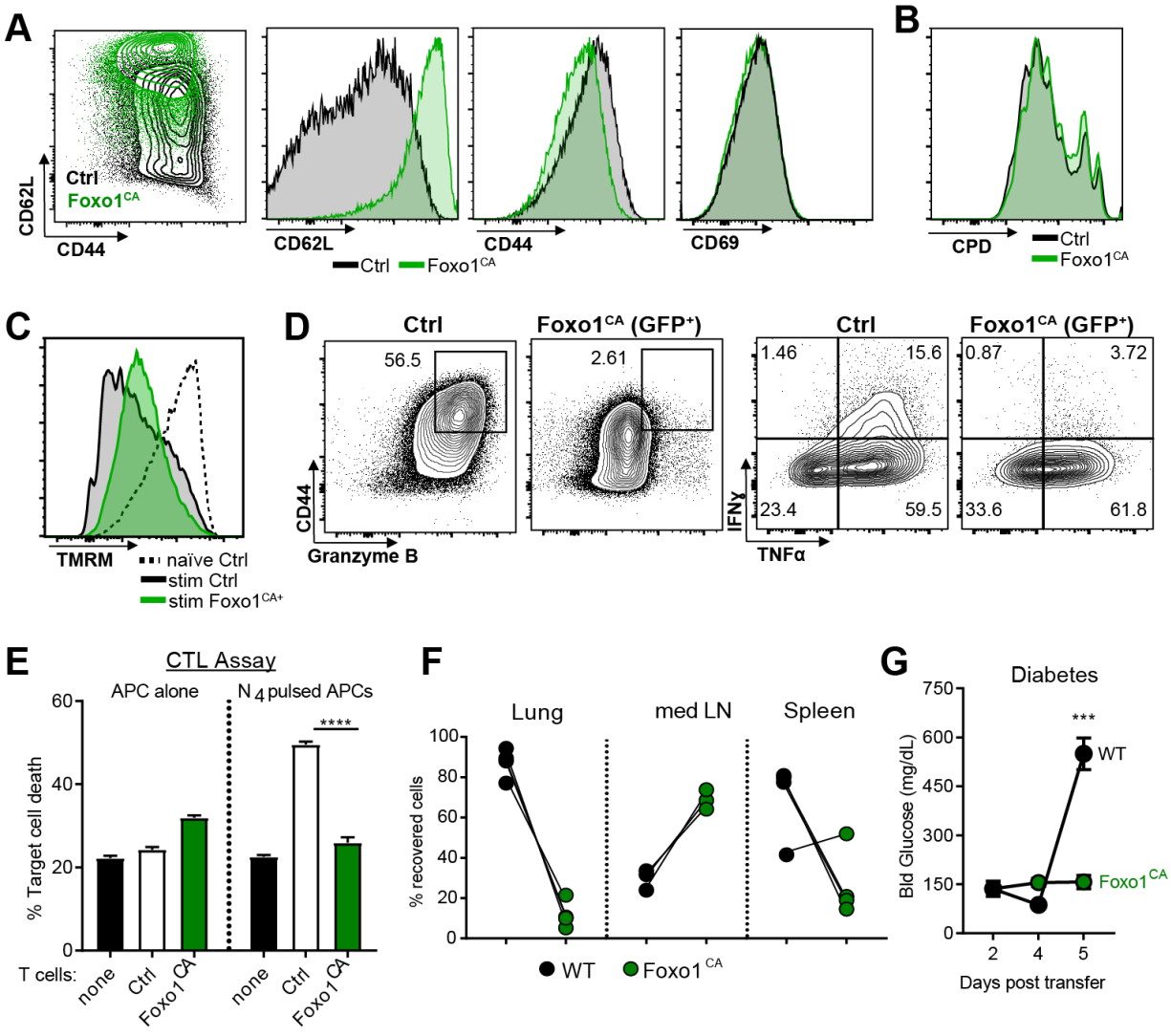

Figure 4.2: Sustained expression of Foxo1 inhibits effector T cell function

A) Representative flow cytometry plots and histograms of CD62L and CD44 expression by gated $CD8^+$ T cells 48 hrs after αCD3/CD28 stimulation of sorted naïve $CD8^+$ control or $Foxo1^{CA}$ (GFP^+) T cells. B) Representative histogram of CPD dilution of stimulated purified naive $CD8^+$ T cells. C) Representative histograms TMRM uptake by $TCR\beta^+$ $CD8^+$ T cells. D) Representative flow cytometry plots of cytokine production by gated $TCR\beta^+$ $CD8^+$ T cells 48 hrs after stimulation of purified naive $CD8^+$ T cells with αCD3/CD28 and 4 hrs of PMA/ionomycin/monensin stimulation. E) Graphical analysis of CTL assay, summary of 3 independent experiments. F) Frequency of recovered OT-I $CD8^+$ T cells transferred into WT recipients, 7 days after intranasal infection with VSV-OVA. G) Blood glucose levels of RIP-mOVA mice injected with WT or dLck-cre $Foxo1^{CA}$ OT-I $CD8^+$ T cells. Significance determined by students t-test , ***$p < 0.001$.

Identification of novel molecular pathways regulated by Foxo1

To identify the transcriptional pathways regulated by Foxo1 we performed RNA-seq using conditions similar to our *in vitro* stimulations (Fig 4.2A). Naïve control or Foxo1^{CA} (GFP^{+}) CD8^{+} T cells were sorted and lysed directly post-sort for RNA or stimulated for 48 hours with platebound αCD3/CD28 and supplemented IL-2. Principal component analysis (PCA) revealed few differences between naïve samples but striking differences between stimulated control and Foxo1^{CA} samples (Fig 4.3A). We noted 17 differentially expressed (DE) genes between naïve control and naïve Foxo1^{CA} cells, with several genes such as *Gpr55* and *Scl6a19* related to metabolism (Fig 4.3B). The largest differences were found between stimulated control and Foxo1^{CA} CD8^{+} T cells with 1110 DE genes (Fig 4.3B). Interestingly Foxo1^{CA} T cells had DE genes that were both higher and lower expression than control, suggesting that during activation sustained Foxo1 expression both prevents engagement of activation pathways and sustains expression of naïve pathways. Consistent with this hypothesis, examination of the top 300 DE genes revealed naïve samples to have similar gene expression profiles regardless of the Foxo1^{CA} allele (Fig 4.3C). Indeed, we noted high expression of *Sell* (CD62L)*, Il7rα and Ccr7*, genes known to be regulated by Foxo1 that promote the naïve phenotype in T cells (53). For a large subset of genes which normally are upregulated upon stimulation, Foxo1^{CA} T cells failed to upregulate expression and showed similar levels as naïve samples. Foxo1^{CA} T cells had lower expression of genes associated with activation and effector function such as *Ifng*, *Eomes* and *Lta*. Intriguingly, we noted a set of genes which have overall low expression in naïve and stimulated control samples but were upregulated in stimulated Foxo1^{CA} samples. This observation led us to hypothesize that in the absence of Foxo1 inactivation and downstream signaling, alternative pathways of activation are used in an attempt to achieve effector function (Fig 4.3C). Suggestive of this, we observed altered expression of costimulatory and coinhibitory pathways in activated Foxo1^{CA} T cells (Fig 4.4).

To further explore differences between normal inactivation of Foxo1 (control) and sustained expression (Foxo1^{CA}), we focused on genes that were upregulated in either of the stimulated samples compared to each other (Fig 4.3D). Gene Ontology (GO) term enrichment analysis of genes DE between stimulated control and Foxo1^{CA} samples identified several pathways associated with effector function and T cell activation (Fig 4.3E). In agreement with our earlier assessment of reduced effector function in Foxo1^{CA} T cells (Fig 4.2), there was an enrichment for categories such as 'cytokine activity' and 'regulation of cytokine production'. Along with our observations that Foxo1^{CA} cells failed to migrate properly to sites of inflammation (Fig 4.2G), there was enrichment for genes in several 'chemotaxis' and 'inflammatory response' categories.

Lastly, we utilized a published list of genes associated with differentiation of effector T cells (84). Kakaradov and colleagues examined regulation of early activation in CD8^{+} T cells, defining a transcriptional profile which after one division could predict if T cells would become terminal effectors or proceed to become memory cells. This gene list was of particular interest to us because of the early activation timepoint as our data suggest Foxo1^{CA} T cells are hindered in their differentiation as early as 48 hours after stimulation. We noted an enrichment of differentiation associated genes in stimulated control samples compared to stimulated Foxo1^{CA} samples (Fig 4.3E). Thus, these data demonstrate that Foxo1^{CA} T cells fail to differentiate as well as control cells on a molecular level at early timepoints after activation.

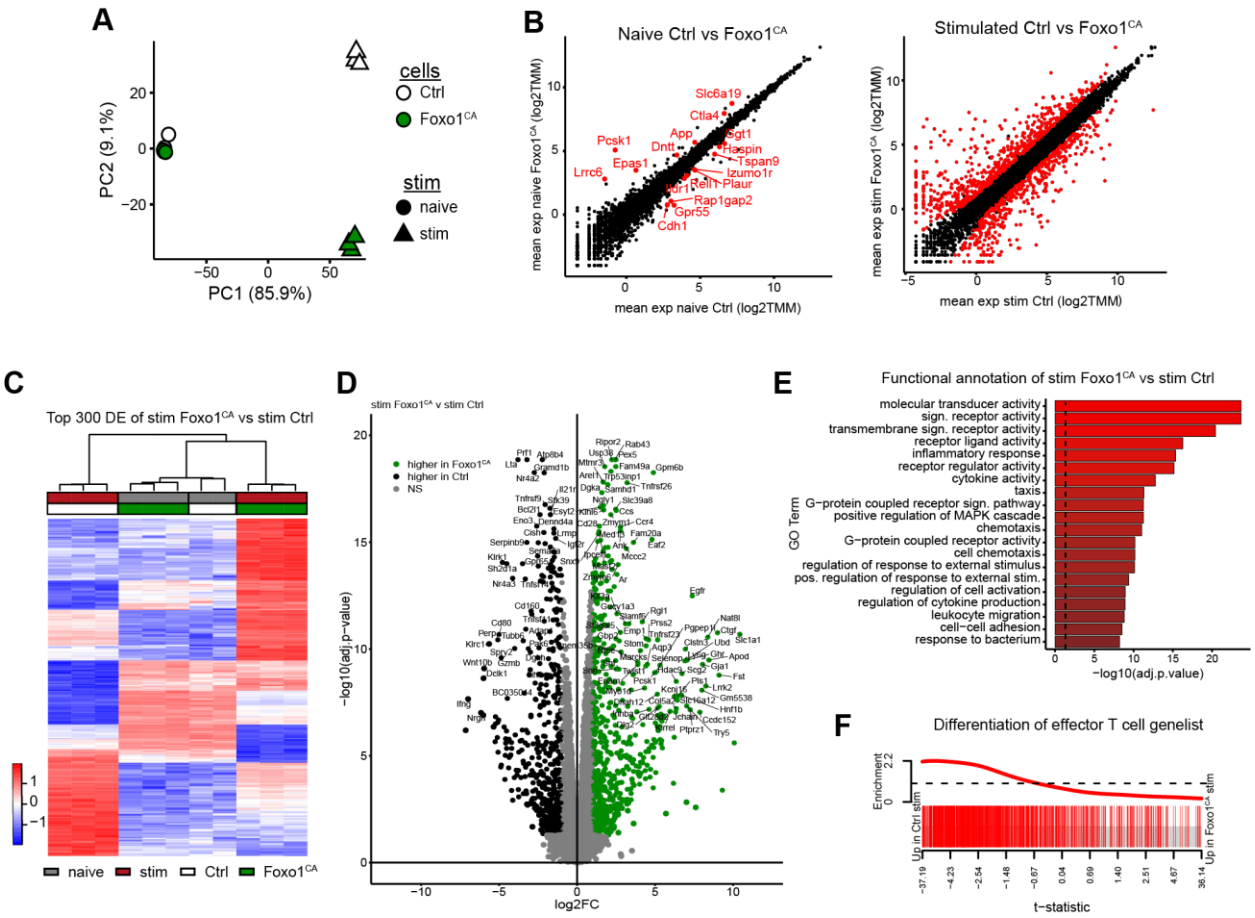

Figure 4.3: Identification of novel molecular pathways regulated by Foxo1

A) PCA of RNA-seq data from control or Foxo1^{CA} (GFP^{+}) sorted naive CD8^{+} T cells ex vivo or stimulated for 48 hrs with platebound αCD3/CD28. B) (Left) Graphed mean expression of genes naïve Ctrl vs Foxo1^{CA}. (Right) stimulated Ctrl vs stimulated Foxo1^{CA} samples. DE genes highlighted in red. C) Heatmap and hierarchical clustering of RNA-seq samples based on the 300 most variably expressed genes between stimulated samples. D) Volcano plot of DE genes between stimulated Ctrl vs Foxo1^{CA} with a log 2 fold change cutoff. E) GO term enrichment for DE genes between stimulated Ctrl vs Foxo1^{CA}. Dashed line represents adjusted p value of 0.05. F) Enrichment of genes associated with CD8^{+} T cell differentiation set along ranked lists of indicated pairwise comparisons (84).

Inactivation of Foxo1 coordinates changes in costimulatory and transcription factor expression during T cell activation

Of the DE genes we observed between stimulated control and Foxo1^{CA} T cells (Fig 4.3D), several potential Foxo1 targets were identified. First we noted several costimulatory genes with altered expression in Foxo1^{CA} cells such as *Ctla4, Cd28* and several TNF receptor family members (Fig 4.3D). Examining a GO term enrichment 'costimulatory' category we noted that stimulated Foxo1^{CA} T cells showed enhanced expression of several costimulatory genes such as *Cd5* and *Cd28* (Fig 4.4A). To confirm these RNA-seq results we utilized flow cytometry to analyzed expression of various costimulatory/coinhibitory markers on stimulated control and Foxo1^{CA} T cells (Fig 4.4B). We noted increased expression of the costimulatory receptor CD28 and the coinhibitory receptor CTLA4 in activated Foxo1^{CA} T cells compared to controls. Conversely, we noted reduced expression of costimulatory receptors OX40, GITR and 41BB. These data suggest that Foxo1^{CA} cells are unable to receive proper costimulatory and coinhibitory signals, perhaps helping to identify one mechanism by which Foxo1^{CA} T cells fail to properly differentiate into effector T cells.

Second, we noted altered expression of interferon regulatory factors (IRF) family members; specifically *Irf4* and *Irf8,* which have been associated with T cell activation and function (Fig 4.4C). IRF4 has been shown to regulate the magnitude of CD8^{+} T cell response via TCR affinity (85, 86) and regulation of T helper differentiation (87). Although less well studied and with conflicting results, a role for IRF8 in T cell differentiation has been demonstrated with loss of IRF8 both inhibiting (88) and promoting inflammation (89). RNA-seq revealed similar levels of *Irf4* and *Irf8* transcripts in naïve samples but a specific loss of IRF8 upregulation in stimulated Foxo1^{CA} T cells (Fig 4.4C). We confirmed these findings by intracellular staining of sorted naïve control or Foxo1^{CA} T cells stimulated for various times (Fig 4.4D). To determine pathways which Foxo1 could be regulating through IRF8 modulation we set out to examine effector T cell function in the absence of IRF8.

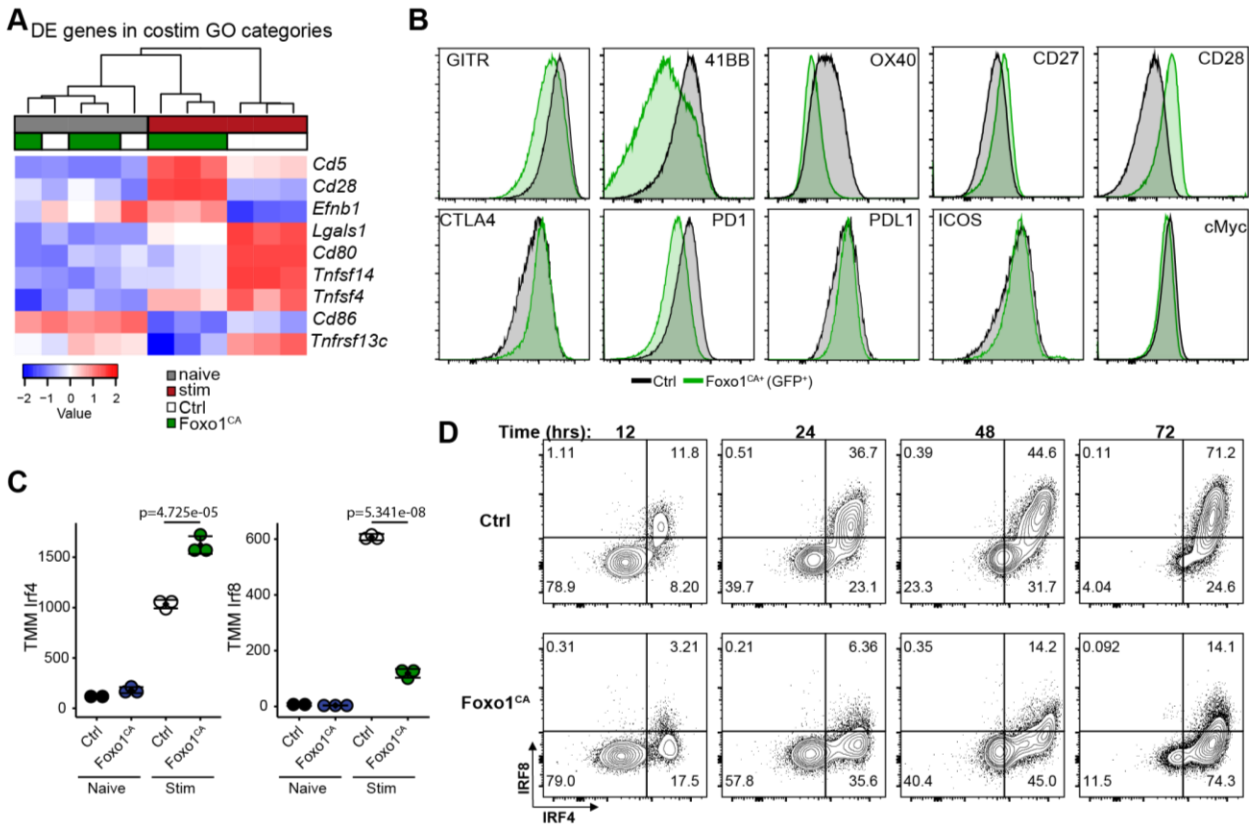

Figure 4.4: Inactivation of Foxo1 coordinates changes in costimulatory and transcription factor expression during T cell activation

A) Heatmap and hierarchical clustering of RNA-seq samples based on costimulatory GO term functional categories. B) Representative histograms of stimulated Ctrl or Foxo1^{CA} CD8^{+} T cells for indicated costimulatory markers. C) Graphical analysis of normalized transcript reads for IRF4 or IRF8 from RNA-seq data. D) Representative flow cytometry plots of IRF4 and IRF8 expression in sorted naïve Ctrl or Foxo1^{CA} CD8^{+} T cells stimulated for indicated timepoints with platebound αCD3/CD28.

Lack of IRF8 does not recapitulate Foxo1^{CA}-driven CD8^{+} T cell dysregulation

We crossed CD4-cre x IRF8 floxed mice (IRF8^{KO}) to generate mice selectively deficient for IRF8 in CD4^{+} and CD8^{+} T cells (90). IRF8^{KO} mice were healthy with comparable frequencies of splenic naïve and effector CD8^{+} T cells as littermate controls (Fig 4.5A). Confirming cre-mediated recombination of the floxed allele, stimulation IRF8^{KO} CD8^{+} T cells lacked IRF8 but not IRF4 upregulation (Fig 4.5B). Stimulated IRF8^{KO} and control CD8^{+} T cells were similarly activated, with high expression of CD25, CD44 and loss of CD62L expression (Fig 4.5C and not shown). Together these data demonstrate that, unlike Foxo1^{CA} T cells, IRF8^{KO} T cells are not skewed towards a naïve phenotype and are capable of *in vitro* activation. To continue investigating potential transcriptional regulation of IRF8 by Foxo1, we generated IRF8^{KO} samples for RNAseq. Sorted naïve control or IRF8^{KO} CD8^{+} T cells were lysed directly post-sort for RNA or stimulated for 48 hours with platebound αCD3/CD28 and supplemented IL-2. Principal component analysis (PCA) revealed little difference between control and IRF8^{KO} samples regardless of activation (Fig 4.5D). Comparing stimulated control and IRF8^{KO} samples, we identified 45 DE genes, substantially fewer DE genes than identified in the Foxo1^{CA} RNA-seq (Fig 4.5E). To compare IRF8 and Foxo1 regulation, we examined overlap of DE genes between stimulated Foxo1^{CA} and stimulated IRF8^{KO} CD8^{+} T cells. Only 19 DE genes overlapped between the samples, with no discernable patterns of function among the identified genes (Fig 4.5F). Together these data demonstrate that lack of IRF8 signaling does not recapitulate phenotypic or functional consequences of sustained Foxo1 expression as observed in Foxo1^{CA} cells. Although these data do not elucidate the relationship between Foxo1 and IRF8, it does not necessarily discount a potential regulatory mechanism. Indeed, it has been demonstrated that IRF4 and IRF8 have similar molecular structures and have compensatory mechanisms (91). It is possible that T cells lacking IRF8 compensation for effector T cell functions by utilizing IRF4 protein at known sites of IRF8 binding. We observed increased IRF4 RNA transcripts in Foxo1^{CA} CD8^{+} T cells compared to controls (Fig 4.4C), providing some evidence supportive of this

hypothesis. Future studies will examine similarities of Foxo1^{CA} T cells and T cells lacking both IRF4 and IRF8. Additionally we have developed plasmids and protocols to express IRF8 in T cells, thus potentially identifying pathways in which re-expression of IRF8 restores effector function in Foxo1^{CA} CD8^{+} T cells.

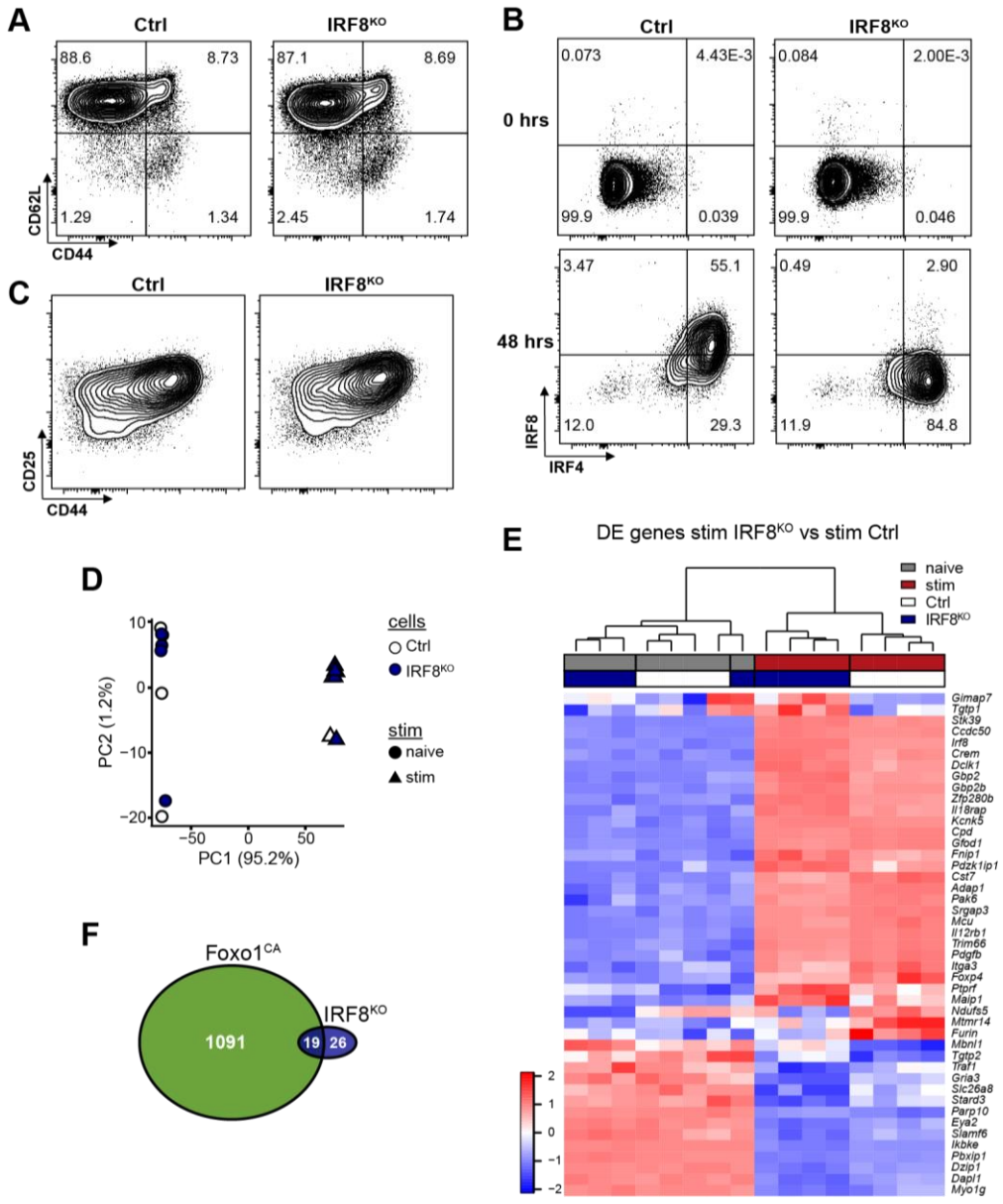

Figure 4.5: Lack of IRF8 does not recapitulate Foxo1^{CA}-driven CD8^{+} T cell dysregulation

A) Representative flow cytometry plots of CD62L and CD44 expression in splenic CD8^{+} T cells from Ctrl or CD4cre^{+} IRF8$^{fl/fl}$ (IRF8^{KO}) mice. B) Representative flow cytometry plots of IRF4 and IRF8 expression in sorted naïve Ctrl or IRF8^{KO} CD8^{+} T cells stimulated for indicated times with platebound αCD3/CD28. C) Representative flow cytometry plots of CD25 and CD44 expression in sorted naïve Ctrl or Foxo1^{CA} CD8^{+} T cells stimulated for 48 hrs with platebound αCD3/CD28. D) PCA of RNA-seq data from Ctrl or IRF8^{KO} naive CD8^{+} T cells ex vivo or stimulated for 48 hrs with platebound αCD3/CD28 in the presence of IL-2 from 4 individual mice. E) Heatmap and hierarchical clustering of RNA-seq samples based on the 300 most variable expressed genes between stimulated samples. F) Venn diagram depicting overlap of DE genes from stimulated Foxo1^{CA} vs stimulated IRF8^{KO} RNA-seq samples.

Discussion:

The data presented here highlight the importance of Foxo1 inactivation during $CD8^+$ T cell differentiation and acquisition of effector function. By using a constitutively active form of Foxo1 we show that $CD4^+$ and $CD8^+$ T cells are skewed towards a naïve phenotype at baseline in dLck-cre $Foxo1^{CA}$ mice. In agreement with these observations, knockout studies have demonstrated that Foxo1 promotes homeostasis of naïve T cells through the positive regulation of CD62L, IL-7Rα and CCR7 (53, 60). Our data confirm these findings but utilize a mouse model of continued activation of Foxo1 rather than its absence. Additionally, we show that continued activation of Foxo1 also inhibited generation of T_R, with few recombined $Foxo1^{CA}$ T_R observed in dLck-cre $Foxo1^{CA}$ mice. In concordance with these observations, using both knockout studies and the $Foxo1^{CA}$ allele, Li and colleagues have demonstrated the importance of Foxo1 in promoting thymic generation of T_R and its role in regulating the transition between cT_R and eT_R (29, 44). Together these data demonstrate that Foxo1 helps maintain a naïve phenotype in both conventional $\alpha\beta$ T cells and $Foxp3^+$ regulatory T cells.

Given its role in promoting a naïve phenotype, we hypothesized that sustained activation of Foxo1 would inhibit effector T cell function. *In vitro* and *in vivo* assays revealed that $Foxo1^{CA}$ $CD8^+$ T cells can be activated but are defective in their ability to differentiate into effector T cells. RNA-seq analysis uncovered a unique set of genes potentially regulated by Foxo1, including costimulatory and coinhibitory receptors and IRF family members. Future studies will examine the relationship between these potential targets and their ability to regulate $CD8^+$ effector T cell function.

Although the data are not included in this dissertation, we also examined how sustained expression of Foxo1 alters $CD4^+$ T cell activation. Although both $CD4^+$ and $CD8^+$ $Foxo1^{CA}$ T cells have overlapping defects in effector function, the degree of change from control cells varied. For example, $CD4^+$ $Foxo1^{CA}$ T cells displayed more drastic alterations in costimulatory receptor and

IRF8 expression than CD8$^+$ Foxo1^{CA} T cells. On the other hand, CD8$^+$ Foxo1^{CA} T cells failed to make select cytokines but CD4$^+$ Foxo1^{CA} T cells only had reduced cytokine production. These observations highlight the temporal and functional differences between CD4$^+$ and CD8$^+$ T cells during activation and suggest potential differential regulation by Foxo1. Additionally, studies from collaborators identified Foxo1 as a driver of CD4$^+$ T cell maintenance through regulation of Myc and IL-2 (71). Newton *et al.* demonstrated that Foxo1 activation drives a decrease in IL-2Rβ expression, which reduced pStat5 signaling needed for upregulation of Myc. Lack of this signaling pathway resulted in decreased cellular cholesterol accumulation which facilitates immunological synapse formation and proliferation. Although we have not experimentally examined metabolic and cellular fitness in Foxo1^{CA} CD8$^+$ T cells, these pathways were not identified in our RNA-seq analysis as significantly different. These data lead us to speculate that there are potentially divergent pathways of Foxo1 regulation in early activation of CD4$^+$ versus CD8$^+$ T cells. Indeed, other PI3K regulated transcription factors are known to have varied roles in regulating cell function. For example, PI3K signaling induces expression of T box transcription factor (Tbet) which plays a vital role in regulating differentiation and function of T cells, B cells, NKT and ILCs (92). CD8$^+$ T cells have varied expression of Tbet throughout their lifetime, which helps direct their transition between naïve, effector and memory phenotypes. However expression of Tbet in CD4$^+$ T cells is less transient with sustained expression promoting Th1 differentiation program while inhibiting other Th genomic profiles (93). Expression of Foxo1 is also varied depending on the effector status of CD8$^+$ T cells, with long-lived memory effectors having higher expression than short-lived effectors. And Foxo1 has been shown to repress Tbet expression in CD8$^+$ T cells (75) but a potential role in regulating Tbet in CD4$^+$ T cells has not been determined. These observations highlight the complex pathways in which PI3K signaling regulates T cell subset activation and function.

Chapter 5:

Dynamic expression of Id3 defines the stepwise differentiation of tissue-resident regulatory T cells

Introduction

Several recent studies have highlighted the phenotypic and functional heterogeneity of T_R cells during both steady state and inflammation (22, 25, 28, 94). We and others have shown that at steady state in lymphoid organs T_R can be broadly divided by expression of CD44 and CD62L into distinct subsets which differ in their localization, dependence on IL-2, and extent of PI3K signaling (26, 28). Moreover, $CD44^{hi}CD62L^{lo}$ effector (e)T_R display diverse expression of transcription factors and chemokine receptors that promote their migration to inflamed tissues and their response to different types of inflammatory signals (25, 31). Accordingly, T_R found in nonlymphoid tissues have a distinct molecular profile that includes high expression of Gata3 and ST2 (the IL-33R), and are functionally equipped to suppress inflammation at barrier sites (30, 95). Although these data highlight the anatomical, functional and molecular diversity of T_R, the pathways by which these T_R populations differentiate have not been completely defined.

The inhibitors of DNA binding (Id) proteins have been extensively studied in lymphocyte development (96, 97). Studies of $CD8^+$ effector T cells revealed that Id2 and Id3 are powerful transcriptional regulators of differentiation that are dynamically regulated during T cell activation and effector/memory T cell differentiation (43, 98). Id proteins regulate the immune system through their modulation of E protein function. E proteins are a family of four proteins, E2-2, HEB and splice variants E12, E47, which act as both transcriptional activators or repressors (96). E proteins function by forming homo or heterodiamers through their bHLH domains and binding to E box consensus sequences in DNA. E proteins are essential regulators of both B and T cell maturation and development (96). Id proteins lack DNA binding domains and function

by heterodiamerizing with an E protein and preventing E protein DNA binding. Through their regulation of E protein function, Id2 and Id3 help to control expression of genes essential for $CD8^+$ effector cell differentiation and survival such as *Tcf7*, *Tbx21*, *Bcl2* and *Klrg1* (99, 100). Although less well studied, Id proteins have been shown to have essential roles in $CD4^+$ T cell function. For instance, Id2 and Id3 are essential for T_R maintenance and function, with T_R lacking both Id2 and Id3 having impaired proliferation and survival (42). In T_R, Id3 helps to stabilize Foxp3 through restriction of the E protein E47 and its downstream targets Spi-B and SOCS3 (101). However, Id3 expression is not uniform in T_R, and distinct populations of $Id3^+$ and $Id3^-$ have been identified (42, 102). In this study, we show that Id3 is dynamically regulated in T_R, and that progressive loss of Id3 correlates with the stepwise differentiation of a highly-functional T_R population localized primarily in non-lymphoid tissues.

Results

Id3 is dynamically expressed in T_R and regulated by TCR signaling

To examine Id3 expression in T_R, we generated Id3-GFP x Foxp3-mRFP double reporter mice. In agreement with previously published reports, most $CD4^+$ T cells in spleen and LNs were $Id3^+$ (42, 102). However, we noted a subset of $Id3^-$ cells in both $Foxp3^+$ T_R and $Foxp3^-$ conventional $CD4^+$ T cell populations (Fig 5.1A). Within T_R, the $Id3^-$ population fell exclusively within the $CD44^{hi}$ $CD62L^{lo}$ eT_R compartment (28), whereas $Id3^+$ T_R were found in both the $CD44^{lo}$ $CD62L^{hi}$ central (c)T_R and eT_R compartments (Fig 5.1B). Thus, in SLOs T_R can be divided into three distinct subsets based on Id3, CD62L and CD44 expression, $Id3^+$ cT_R, $Id3^+$ eT_R or $Id3^-$ eT_R. Within the $Id3^+$ T_R populations $Id3^+$ cT_R had higher Id3 expression than $Id3^+$ eT_R measured by GFP mean fluorescence intensity (Fig 5.1B), leading us to hypothesize that T_R may downregulate Id3 as they transition during their activation and differentiation from cT_R into eT_R. Indeed, Id3 expression can be downregulated by TCR signaling (42), and we observed a loss of Id3 expression in the T_R compartment correlating with the strength of TCR stimulation

when cells were activated with different concentrations of platebound αCD3/28 (data not shown). Furthermore, inhibiting either the MAP-kinase/Erk or PI3-kinase/mTOR signaling pathways blocked Id3 downregulation in T_R (Fig 5.1C), consistent with reports that eT_R development requires TCR stimulation, mTOR signaling and the PI3-kinase-dependent inactivation of the transcription factor Foxo1 (28, 29, 103).

To more precisely define the developmental relationship between these T_R subsets, we utilized an adoptive transfer model in which T_R stimulation and expansion depends on TCR:MHCII interactions (104). For this we sorted $Id3^+$ cT_R, $Id3^+$ eT_R or $Id3^-$ eT_R from spleen and LNs of reporter mice and transferred individual T_R populations into RAG1-deficient animals, and evaluated the phenotype and expansion of transferred T_R after 2 weeks. Importantly, we did not observe any difference in the extent of Foxp3 expression between the T_R populations upon their recovery, which varied between ~30-80% in different experiments (not shown). Transferred $Id3^+$ cT_R gave rise to all three subsets, with some cells retaining Id3 and CD62L expression but the majority converting into $Id3^-$ eT_R (Fig 5.1D). The bulk of $Id3^+$ eT_R downregulated Id3, with no cells regaining CD62L expression, whereas $Id3^-$ eT_R did not give rise to either of the other populations, indicating that these cells are likely a terminally differentiated population. Thus, $Id3^-$ eT_R appear to develop from $Id3^+$ cT_R in a stepwise manner during activation, with $Id3^+$ eT_R acting as an intermediate population.

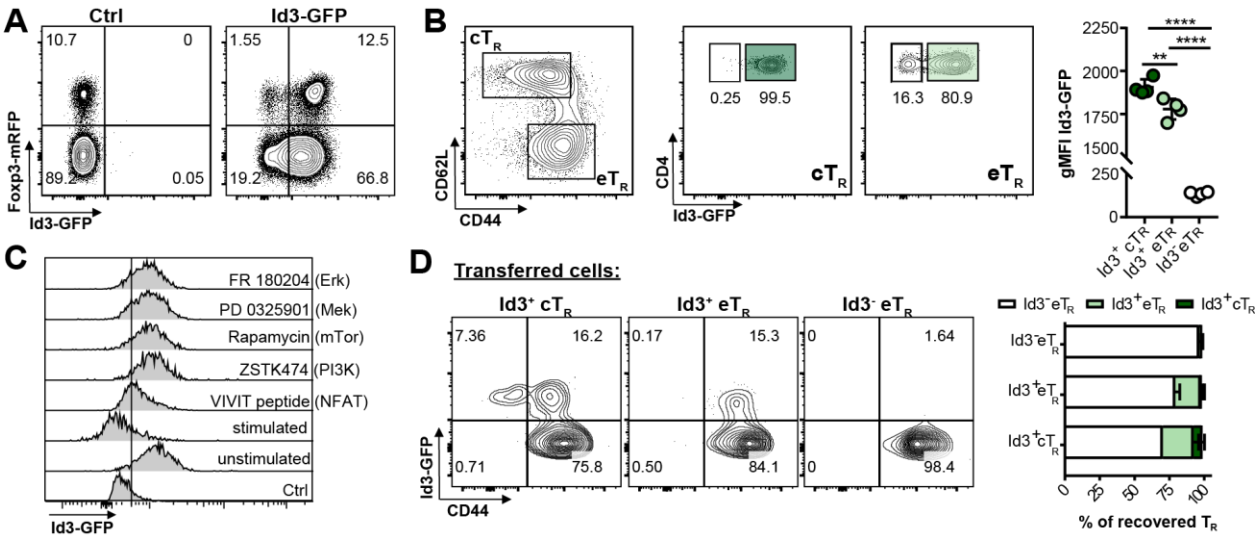

Figure 5.1: Id3 is dynamically expressed in T_R and regulated by TCR signaling

A) Representative flow cytometry plots of Id3-GFP and Foxp3-RFP expression by gated splenic TCRβ$^+$ CD4$^+$ T cells. B) Representative flow cytometry analysis of Id3-GFP expression by splenic CD44^{lo}CD62L^{hi} cT_R and CD44^{hi}CD62L^{lo} eT_R gated as indicated. (Bottom left) Graphical analysis of geometric mean fluorescence intensity (gMF)I of Id3-GFP in each of the three gated T_R populations. C) Representative flow cytometry plots of Id3-GFP expression by gated splenic TCRβ$^+$ CD4$^+$ Foxp3$^+$ T_R 66 hrs after stimulation of purified CD4$^+$ T cells in the presence or absence of the idicated inhibitors, representative of 2 independent experiments. D) Representative flow cytometry plots and graphical analysis of CD44 and Id3-GFP expression by gated TCRβ$^+$CD4$^+$Foxp3$^+$ T_R recovered from the LNs of RAG1-deficient mice 2 weeks after transfer of the indicated T_R population. Data are a summary of 3 independent experiments, 3-5 mice per group total. Significance determined by one way ANOVA with Tukey's post-test for pairwise comparisons, **p < 0.01, ****p < 0.0001

Id3$^-$ eT$_R$ express inhibitory markers and are highly suppressive

To explore the phenotypic and functional differences between these three subsets of T$_R$, we assessed expression of the T$_R$-associated surface markers on each population of splenic T$_R$. In agreement with previously published data, cT$_R$ and eT$_R$ showed distinct phenotypes, with eT$_R$ having lower expression of the high affinity IL-2 receptor component CD25, but higher levels of the activation and functional surface markers ICOS, KLRG1, TIGIT, GITR and CTLA4 (Fig 5.2A) (28, 29). Moreover, within the eT$_R$ compartment the Id3$^-$ T$_R$ had higher expression of activation and inhibitory molecules than their Id3$^+$ T$_R$ counterparts, but had the lowest expression of CD25. As our lab previously described (28), elevated expression of ICOS and diminished expression of CD25 suggests that Id3$^-$ eT$_R$ are less dependent on IL-2 for their homeostatic maintenance, and instead likely rely on continued ICOS signaling. Additionally, increased expression of these T$_R$ functional molecules correlated with enhanced *in vitro* suppressive activity of Id3$^-$ eT$_R$ compared with either Id3$^+$ cT$_R$ or Id3$^+$ eT$_R$ (Fig 5.2B).

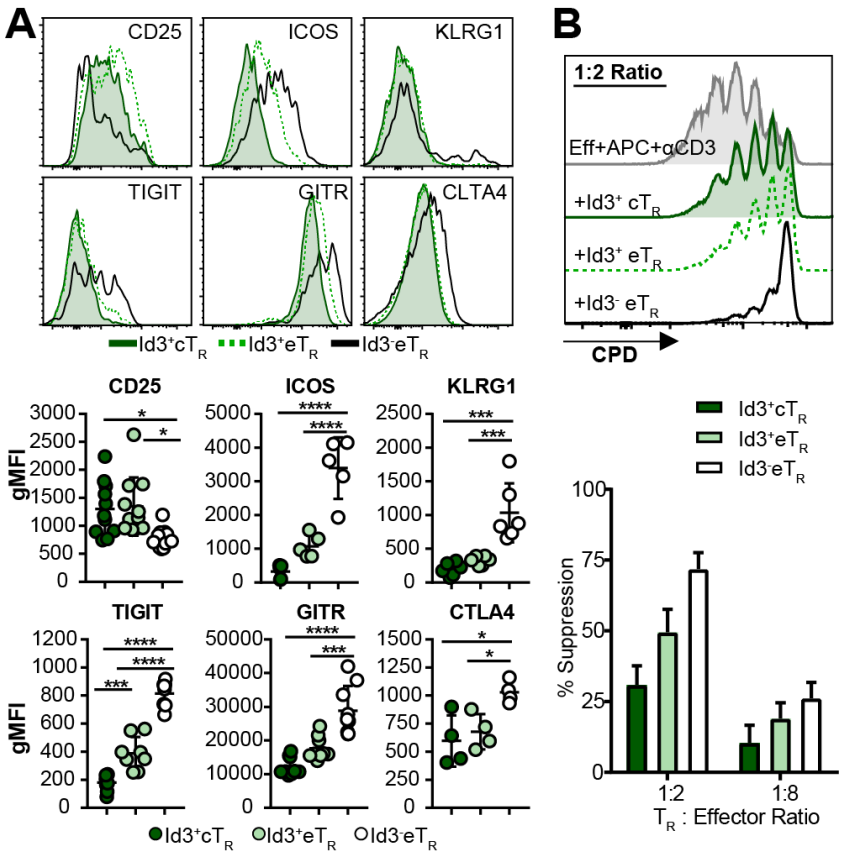

Figure 5.2: Id3$^-$ eT$_R$ express inhibitory markers and are highly suppressive

A) (Top) Representative flow cytometry histograms. (Bottom) Graphical analysis of expression of the indicated markers by gated splenic T$_R$ populations. B) (Top) Representative flow cytometry analysis of cell proliferation dye (CPD) dilution by CD4$^+$Foxp3$^-$ effector T cells stimulated with or without the indicated T$_R$ populations. (Bottom) Graphical analysis of suppression by each of the indicated populations, n=3. Significance determined by one way ANOVA with Tukey's post-test for pairwise comparisons, *p <0.05, ***p < 0.001, ****p < 0.0001

Transcriptional profiling highlights the stepwise differentiation of Id3$^-$ eT$_R$

To identify and compare their unique transcriptional profiles, we performed RNA-seq on sorted Id3$^+$ cT$_R$, Id3$^+$ eT$_R$ and Id3$^-$ eT$_R$ from spleen or LNs of Id3-GFP x Foxp3-mRFP reporter mice. Although there was little difference between LN and spleen samples, PCA showed that each of the three T$_R$ populations were transcriptionally distinct (Fig 5.3A), and accordingly we identified 1,672 significantly DE genes between the three T$_R$ populations (Fig 5.3B). The largest differences were found between Id3$^-$ eT$_R$ and Id3$^+$ cT$_R$ with 1,471 DE genes, whereas only 474 genes differed between Id3$^+$ and Id3$^-$ eT$_R$ (Fig 5.3B). Interestingly among the DE genes we observed a reciprocal increase in Id2 expression as T$_R$ lose Id3 (Fig 5.3C). This differential Id expression in T$_R$ is similar to what occurs in CD8$^+$ T cells, which upregulate Id2 and downregulate Id3 while becoming activated and gaining effector function (43, 98). This suggests that as T$_R$ downregulate Id3, the closely related Id2 may take over some of its functions while also driving a unique E-protein-dependent signature promoting eT$_R$ development. Consistent with the stepwise differentiation model we propose for these populations, examination of the 300 most DE genes across the three T$_R$ subsets (based on highest F-value) showed that both up and downregulated genes were generally expressed in a gradient fashion, with expression in Id3$^+$ eT$_R$ falling between that of Id3$^+$ cT$_R$ and Id3$^-$ eT$_R$ (Fig 5.3D-E). Moreover, in accordance with our prior phenotypic analysis and their enhanced suppressive activity, Id3$^-$ eT$_R$ showed elevated expression of known T$_R$ function genes, including *Il10, Ctla4, Pdcd1, Tnfrsf4, Lag3 and Ebi3* (Fig 5.3F). To further validate our RNA-seq results, we confirmed differential expression of several T$_R$-associated genes by flow cytometry (Fig 5.4). GO term enrichment analysis of genes DE between Id3$^+$ eT$_R$ and Id3$^-$ eT$_R$ identified specific molecular pathways altered between these closely related populations (Fig 5.3G). The top six enriched categories all related to cytokine and chemokine receptor signaling, with Id3$^-$ eT$_R$ expressing high levels of receptors indicating that they can tune their activity in response to key

inflammatory cytokines such as IL-1, IL-18, IL-23, and IL-25 (Fig 5.3H). Moreover, among the DE chemokine receptors, $Id3^{-}$ eT_R had the highest expression and subsequent responsiveness to chemokines that promote lymphocyte migration to inflamed tissues, such as *Ccr4 and Cxcr3* (Fig 3H-I) (25). Thus, $Id3^{-}$ eT_R have a unique molecular profile indicative of their development from $Id3^{+}$ T_R precursors, their elevated suppressive function and altered migratory capacity.

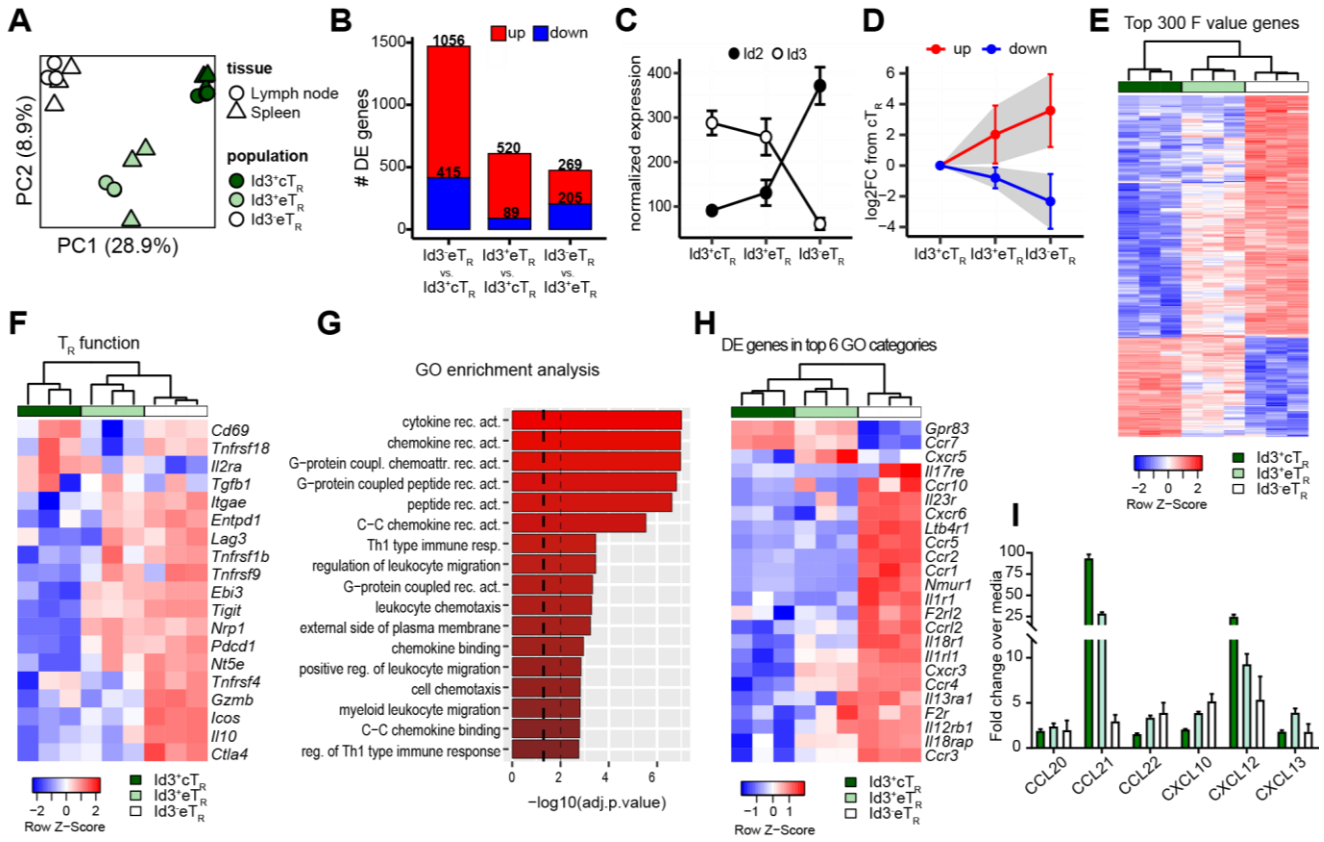

Figure 5.3: Transcriptional profiling highlights the stepwise differentiation of Id3$^-$ eT$_R$

A) PCA of RNA-seq data from LN and splenic Id3$^+$ cT$_R$, Id3$^+$ eT$_R$ and Id3$^-$ eT$_R$ populations sorted from three individual mice. B) Bar graphs showing the number of differentially expressed genes (adj.p.value < 0.05 and log2FC >1) for each of the indicated pairwise comparisons. C) Graphical analysis of normalized transcript reads for Id2 or Id3 from RNA-seq data. D) The 300 most differentially expressed genes (determined by F value) were split into the upregulated (red) and downregulated (blue) fractions based expression in Id3$^-$ eT$_R$ vs Id3$^+$ cT$_R$. Graph shows the mean log2FC compared to Id3$^+$ cT$_R$ for both eT$_R$ populations. Error bars and shaded area represent 1x SD. E) Heatmap and hierarchical clustering of splenic RNA-seq samples based on the 300 most variably expressed genes. F) Heatmap and hierarchical clustering of splenic RNA-seq samples based on T$_R$ signature genes identified in reference (30). G) GO term enrichment analysis for DE genes of Id3$^-$ eT$_R$ vs. Id3$^+$ eT$_R$. Dashed lines represent adjusted p values of 0.05 and 0.01. H) Heatmap and hierarchical clustering of splenic RNA-seq samples based on DE genes found in the top 6 GO functional categories enriched in the comparison of Id3$^+$ and Id3$^-$ eT$_R$. I) Graphical analysis of chemotaxis assay.

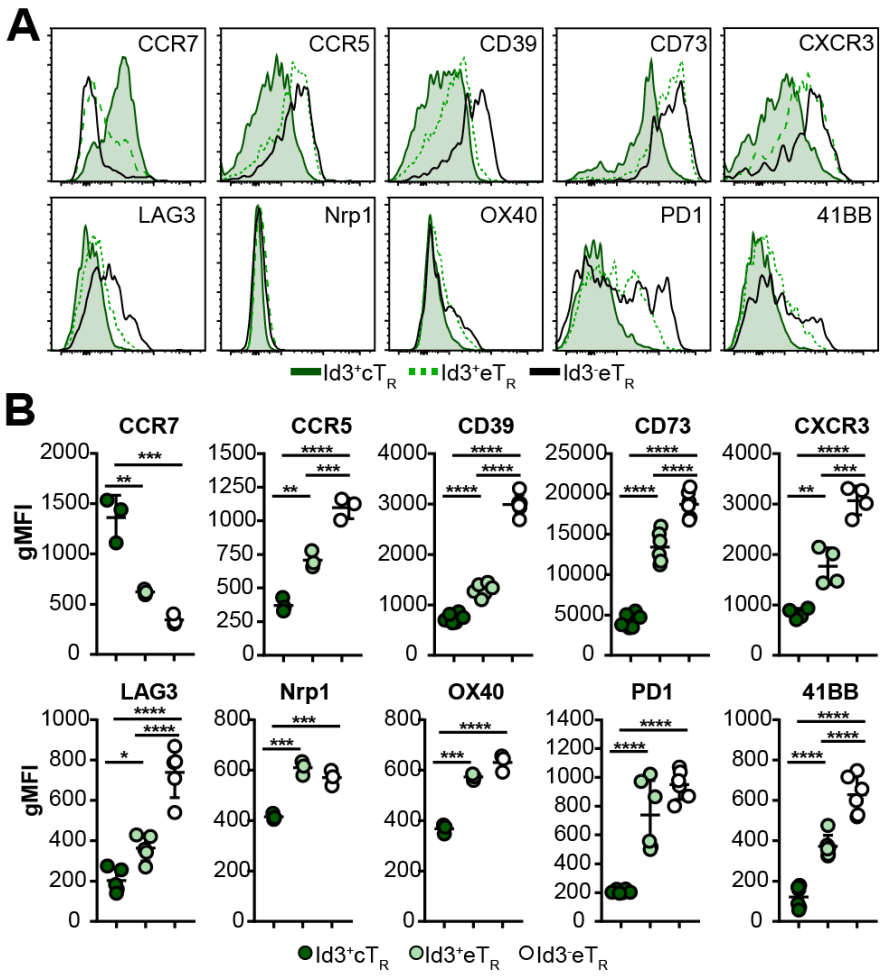

Figure 5.4: Flow cytometry validation of RNA-seq targets

A) Representative flow cytometry histograms. B) Graphical analysis of expression of the indicated markers by gated splenic T_R populations. Significance determined by one way ANOVA with Tukey's post-test for pairwise comparisons, *p <0.05, **p < 0.01, ***p < 0.001, ****p < 0.0001

Id3$^-$ T_R are enriched and resident in non-lymphoid tissues

In contrast to their elevated expression of inflammatory chemokine receptors, Id3$^-$ eT_R had the lowest expression of *Ccr7* and *S1pr1* which function together to promote T_R recirculation through SLOs (59) (Fig 5.3H). Additionally, expression of CD103 and CD69, which together act to retain tissue-resident memory T($_{RM}$) cells in non-lymphoid sites, was strongly enriched in Id3$^-$ eT_R, suggesting these cells may be tissue-resident (Fig 5.5A) (10, 11). Indeed, utilizing published gene signatures of CD8$^+$ T_{RM} or circulating memory T cells (105), we found that the CD8$^+$ T_{RM} signature gene set was enriched in Id3$^-$ eT_R compared to either Id3$^+$ cT_R or Id3$^+$ eT_R, whereas the circulating memory gene set was enriched in the Id3$^+$ T_R populations (Fig 5.5B). Several groups have recently identified the ST2 (IL-33R)-Gata3 axis as a key determinant of T_R residency and function in non-lymphoid tissues (30, 95, 106). Accordingly, Id3$^-$ eT_R had the highest expression of all positively associated tissue T_R genes such as *Il1rl1* (ST2), *Gata3*, *Areg*, *Irf4 and Rora*, whereas Id3$^+$ cT_R had the lowest expression of these genes but high expression of negative regulators of tissue residence such as *Tcf7, Klf2* and *Lef1,* and Id3$^+$ eT_R displayed intermediate expression for all of these genes (Fig 5.5C). Consistent with their T_{RM}-like transcriptional signature, Id3$^-$ eT_R were a minority of T_R in LNs and spleen, but their frequency dramatically increased in nonlymphoid tissues, where they highly expressed the T_{RM} surface markers CD103 and CD69 (Fig 5.5D-F). Indeed, tissues such as the fat and skin contained almost exclusively Id3$^-$ eT_R. Of particular note Id3$^-$ eT_R were rarest in the lymph and blood, indicating that Id3$^-$ eT_R do not actively recirculate, but instead are retained as tissue-resident cells in non-lymphoid organs.

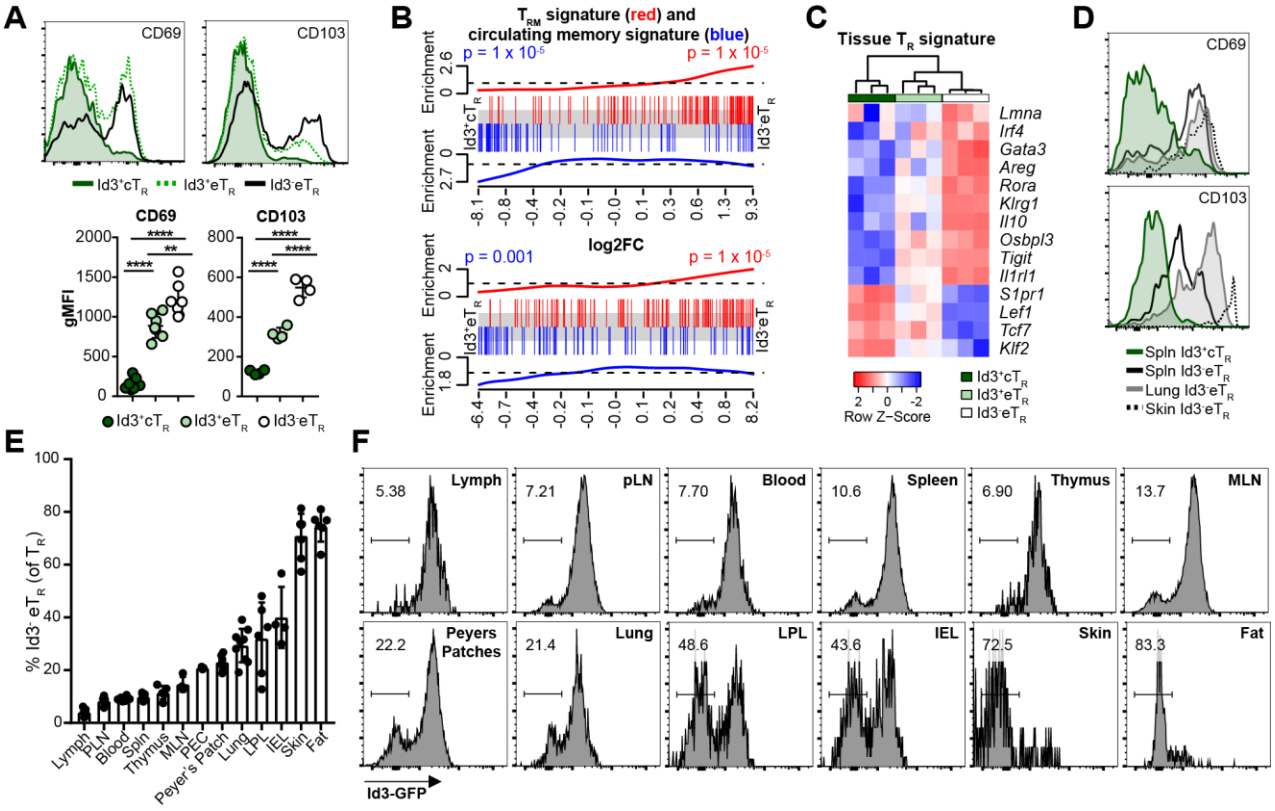

Figure 5.5: Id3$^-$ eT$_R$ are enriched and resident in non-lymphoid tissues

A) Representative flow cytometry histograms and graphical analysis of expression of the CD69 and CD103 by gated splenic T$_R$ populations. B) Enrichment of CD8$^+$ T$_{RM}$ (red) or circulating T cell (blue) gene sets along ranked lists of the indicated pairwise comparisons. C) Heatmap and hierarchical clustering of splenic RNA-seq samples based on ST2$^+$ tissue T$_R$ associated genes. D) Representative flow cytometry plots of CD103 and CD69 expression by gated TCRβ$^+$ CD4$^+$ Foxp3$^+$ T$_R$ in the indicated tissues. E) Graphical analysis of Id3$^-$ eT$_R$ frequency among total T$_R$ in various tissues. F) Representative histograms of GFP expression from various tissues of Id3-GFP x Foxp3-mRFP mice, gated on TCRβ$^+$ CD4$^+$ Foxp3$^+$ T$_R$. Significance determined by one way ANOVA with Tukey's post-test for pairwise comparisons, **p < 0.01, ****p < 0.0001

Discussion

Despite significant interest in tissue-resident T_R, the mechanisms regulating their differentiation and distribution are still poorly defined. Our data show that T_R can be subdivided based on Id3 expression and known markers of cT_R and eT_R into distinct populations, and together our phenotypic, functional, transcriptional and transfer analyses strongly support a stepwise differentiation model in which T_R downregulate Id3 as they progressively gain effector function, tissue homing capacity and residency in non-lymphoid organs. Similarly, Li *et al.* recently proposed a stepwise model for the differentiation of adipose T_R in which activation in the spleen allowed T_R to migrate into the adipose tissue, where IL-33 signaling drove their terminal differentiation and functional specialization (106). High expression of costimulatory receptors such as ICOS and receptors for inflammatory cytokines would also allow $Id3^- eT_R$ to respond to inflammatory signals that enhance Foxp3-mediated transcriptional repression and promote eT_R differentiation and function (61), in part through activation of mTORC1 signaling (103). Although the direct role of Id3 downregulation in the functional differentiation of T_R is still not established, our data highlight the complexity of tissue T_R development, and identify novel molecular pathways that are modulated during their stepwise differentiation.

Chapter 6:

Concluding Remarks

Here, we examined the role of the transcription factor Foxo1 and inhibitor of DNA binding protein, Id3, which are both inactivated downstream of PI3K signaling in αβ T cells. Although the importance of PI3K-AKT-mTOR signaling in T cells has been well established, the far-reaching effects of this pathway are still being interrogated. The experiments herein provide new insight into PI3K regulation of T cell development, effector function and localization. Our data demonstrate that expression of PI3K controlled transcriptional regulators Foxo1 and Id3, are continually fine-tuned during the life span of a T cell. We show that inappropriate activation of Foxo1 during thymic development or after TCR activation hinders T cell development and effector function respectively. Furthermore, we demonstrate that Id3 expression is dynamically regulated during T_R development, activation and tissue-residency.

In additional to both being downregulated upon TCR/PI3K signaling, expression of Foxo1 and Id proteins often track together in peripheral T cells, naïve T cells have high expression of both Foxo1 and Id3 and eT_R have reduced Foxo1 and Id3 expression compared to cT_R ((29) and data in chapter 5). Indeed, T cells undergo immense transcriptional changes during activation and their differentiation into effector cells. Numerous other transcriptional regulators which promote effector function are change expression in T cells upon engagement of PI3K signaling such as Tbet, RORγ, Foxp3 and Gata3. Researchers have been dissecting the complicated web of PI3K signaling for over three decades, yet we still have not discovered all the nuances of this signaling cascade. Insights into this pathway have identified potential therapeutic mechanisms in which the immune system can be manipulated, such as immune checkpoint inhibitors and engineered CAR T cells. Herein, we highlight only two of the numerous transcriptional regulators that work in harmony to elicit a proper immune response

downstream of PI3K signaling. However, few studies have examined potential regulation of Foxo1 by E-proteins/Id and vice versa. Indeed, there are E2A binding sites in the Foxo1 gene and Foxo1 binding sites within the Id3 gene locus (personal observations). These observations highlight the complex and not fully understood roles of players involved in the PI3K signaling cascade. The data herein provide some insight into the intricate roles these two transcriptional regulators, Foxo1 and Id3, play in the PI3K pathway and their regulation of immune tolerance.

References

1. Gascoigne, N., V. Rybakin, O. Acuto, and J. Brzostek. 2016. TCR Signal Strength and T Cell Development. *Annual Review of Cell and Developmental Biology* 32: 327-348.
2. Zúñiga-Pflücker, J. 2004. T-cell development made simple. *Nature Reviews Immunology* 4: 67-72.
3. Han, J. M., S. J. Patterson, and M. K. Levings. 2012. The Role of the PI3K Signaling Pathway in CD4+ T Cell Differentiation and Function. *Frontiers in Immunology* 3: 245.
4. Vanhaesebroeck, B., L. Stephens, and P. Hawkins. 2012. PI3K signalling: the path to discovery and understanding. *Nature Reviews Molecular Cell Biology* 13: 195.
5. Parish, I. A., and S. M. Kaech. 2009. Diversity in CD8(+) T cell differentiation. *Curr Opin Immunol* 21: 291-297.
6. Chang, J. T., J. E. Wherry, and A. W. Goldrath. 2014. Molecular regulation of effector and memory T cell differentiation. *Nature Immunology* 15.
7. Youngblood, B., S. J. Hale, H. T. Kissick, E. Ahn, X. Xu, A. Wieland, K. Araki, E. E. West, H. E. Ghoneim, Y. Fan, P. Dogra, C. W. Davis, B. T. Konieczny, R. Antia, X. Cheng, and R. Ahmed. 2017. Effector CD8 T cells dedifferentiate into long-lived memory cells. *Nature* 552: 404.
8. Akondy, R. S., M. Fitch, S. Edupuganti, S. Yang, H. T. Kissick, K. W. Li, B. A. Youngblood, H. A. Abdelsamed, D. J. McGuire, K. W. Cohen, G. Alexe, S. Nagar, M. M. McCausland, S. Gupta, P. Tata, N. W. Haining, J. M. McElrath, D. Zhang, B. Hu, W. J. Greenleaf, J. J. Goronzy, M. J. Mulligan, M. Hellerstein, and R. Ahmed. 2017. Origin and differentiation of human memory CD8 T cells after vaccination. *Nature* 552: 362.
9. Milner, J. J., and A. W. Goldrath. 2018. Transcriptional programming of tissue-resident memory CD8+ T cells. *Current opinion in immunology* 51: 162-169.
10. Mackay, L. K., A. Rahimpour, J. Z. Ma, N. Collins, A. T. Stock, M. L. Hafon, J. Vega-Ramos, P. Lauzurica, S. N. Mueller, T. Stefanovic, D. C. Tscharke, W. R. Heath, M. Inouye, F. R. Carbone, and T. Gebhardt. 2013. The developmental pathway for CD103(+)CD8+ tissue-resident memory T cells of skin. *Nat Immunol* 14: 1294-1301.
11. Schenkel, J. M., and D. Masopust. 2014. Tissue-resident memory T cells. *Immunity* 41: 886-897.
12. Taniuchi, I. 2018. CD4 Helper and CD8 Cytotoxic T Cell Differentiation. *Annual review of immunology* 36: 579-601.
13. Vinuesa, C. G., M. A. Linterman, D. Yu, and I. C. MacLennan. 2016. Follicular Helper T Cells. *Annual review of immunology* 34: 335-368.
14. Stone, E. L., M. Pepper, C. D. Katayama, Y. M. Kerdiles, C.-Y. Y. Lai, E. Emslie, Y. C. Lin, E. Yang, A. W. Goldrath, M. O. Li, D. A. Cantrell, and S. M. Hedrick. 2015. ICOS coreceptor signaling inactivates the transcription factor FOXO1 to promote Tfh cell differentiation. *Immunity* 42: 239-251.
15. Dardalhon, V., T. Korn, V. K. Kuchroo, and A. C. Anderson. 2008. Role of Th1 and Th17 cells in organ-specific autoimmunity. *Journal of Autoimmunity* 31: 252-256.
16. Walker, J. A., and A. N. J. N. J. McKenzie. 2018. TH2 cell development and function. *Nature reviews. Immunology* 18: 121-133.
17. Sakaguchi, S., N. Sakaguchi, M. Asano, M. Itoh, and M. Toda. 1995. Immunologic self-tolerance maintained by activated T cells expressing IL-2 receptor alpha-chains (CD25). Breakdown of a single mechanism of self-tolerance causes various autoimmune diseases. *Journal of immunology (Baltimore, Md. : 1950)* 155: 1151-1164.
18. Brunkow, M. E., E. W. Jeffery, K. A. Hjerrild, B. Paeper, L. B. Clark, S.-A. Yasayko, E. J. Wilkinson, D. Galas, S. F. Ziegler, and F. Ramsdell. 2001. Disruption of a new forkhead/winged-helix protein, scurfin, results in the fatal lymphoproliferative disorder of the scurfy mouse. *Nature Genetics* 27: 68.
19. Clark, L. B., M. W. Appleby, M. E. Brunkow, J. E. Wilkinson, S. F. Ziegler, and F. Ramsdell. 1999. Cellular and molecular characterization of the scurfy mouse mutant. *Journal of immunology (Baltimore, Md. : 1950)* 162: 2546-2554.
20. Bennett, C. L., J. Christie, F. Ramsdell, M. E. Brunkow, P. J. Ferguson, L. Whitesell, T. E. Kelly, F. T. Saulsbury, P. F. Chance, and H. D. Ochs. 2001. The immune dysregulation, polyendocrinopathy, enteropathy, X-linked syndrome (IPEX) is caused by mutations of FOXP3. *Nature Genetics* 27.

21. Nelson, B. H. 2004. IL-2, Regulatory T Cells, and Tolerance. *The Journal of Immunology* 172: 3983-3988.
22. Josefowicz, S. Z., L. F. Lu, and A. Y. Rudensky. 2012. Regulatory T cells: mechanisms of differentiation and function. *Annu Rev Immunol* 30: 531-564.
23. Nishikawa, H., and S. Sakaguchi. 2014. Regulatory T cells in cancer immunotherapy. *Current Opinion in Immunology* 27: 1-7.
24. Takeuchi, Y., and H. Nishikawa. 2016. Roles of regulatory T cells in cancer immunity. *International Immunology* 28: 401-409.
25. Campbell, D. J. 2015. Control of Regulatory T Cell Migration, Function, and Homeostasis. *J Immunol* 195: 2507-2513.
26. S., S. K., S. Shivani, S. J. Michael, and C. D. J. 2014. Regulatory T-cell homeostasis: steady-state maintenance and modulation during inflammation. *Immunological Reviews* 259: 40-59.
27. Abbas, A. K., E. Trotta, D. R Simeonov, A. Marson, and J. A. Bluestone. 2018. Revisiting IL-2: Biology and therapeutic prospects. *Science immunology* 3.
28. Smigiel, K. S., E. Richards, S. Srivastava, K. R. Thomas, J. C. Dudda, K. D. Klonowski, and D. J. Campbell. 2014. CCR7 provides localized access to IL-2 and defines homeostatically distinct regulatory T cell subsets. *J Exp Med* 211: 121-136.
29. Luo, C. T., W. Liao, S. Dadi, A. Toure, and M. O. Li. 2016. Graded Foxo1 activity in Treg cells differentiates tumour immunity from spontaneous autoimmunity. *Nature* 529: 532-536.
30. Delacher, M., C. D. Imbusch, D. Weichenhan, A. Breiling, A. Hotz-Wagenblatt, U. Trager, A. C. Hofer, D. Kagebein, Q. Wang, F. Frauhammer, J. P. Mallm, K. Bauer, C. Herrmann, P. A. Lang, B. Brors, C. Plass, and M. Feuerer. 2017. Genome-wide DNA-methylation landscape defines specialization of regulatory T cells in tissues. *Nat Immunol* 18: 1160-1172.
31. Gratz, I. K., and D. J. Campbell. 2014. Organ-Specific and Memory Treg Cells: Specificity, Development, Function, and Maintenance. *Frontiers in Immunology* 5: 333.
32. Gratz, I. K., H.-A. Truong, S. Yang, M. M. Maurano, K. Lee, A. K. Abbas, and M. D. Rosenblum. 2013. Cutting Edge: Memory Regulatory T Cells Require IL-7 and Not IL-2 for Their Maintenance in Peripheral Tissues. *The Journal of Immunology* 190: 4483-4487.
33. Sun, I.-H., M.-H. Oh, L. Zhao, C. H. Patel, M. L. Arwood, W. Xu, A. J. Tam, R. L. Blosser, J. Wen, and J. D. Powell. 2018. mTOR Complex 1 Signaling Regulates the Generation and Function of Central and Effector Foxp3+Regulatory T Cells. *The Journal of Immunology* 201: 481-492.
34. Fruman, D. A., H. Chiu, B. D. Hopkins, S. Bagrodia, L. C. Cantley, and R. T. Abraham. 2017. The PI3K Pathway in Human Disease. *Cell* 170: 605-635.
35. So, L., and D. A. Fruman. 2012. PI3K signalling in B- and T-lymphocytes: new developments and therapeutic advances. *The Biochemical journal* 442: 465-481.
36. Szydłowski, M., E. Jabłońska, and P. Juszczyński. 2014. FOXO1 Transcription Factor: A Critical Effector of the PI3K-AKT Axis in B-Cell Development. *International Reviews of Immunology* 33: 146-157.
37. Powell, J. D., K. N. Pollizzi, E. B. Heikamp, and M. R. Horton. 2012. Regulation of Immune Responses by mTOR. *Annual Review of Immunology* 30: 39-68.
38. Newton, R. H., and L. A. Turka. 2012. Regulation of T Cell Homeostasis and Responses by Pten. *Frontiers in Immunology* 3: 151.
39. Bensinger, S. J., P. T. Walsh, J. Zhang, M. Carroll, R. Parsons, J. C. Rathmell, C. B. Thompson, M. A. Burchill, M. A. Farrar, and L. A. Turka. 2004. Distinct IL-2 Receptor Signaling Pattern in CD4+CD25+ Regulatory T Cells. *The Journal of Immunology* 172: 5287-5296.
40. Huynh, A., M. DuPage, B. Priyadharshini, P. T. Sage, J. Quiros, C. M. Borges, N. Townamchai, V. A. Gerriets, J. C. Rathmell, A. H. Sharpe, J. A. Bluestone, and L. A. Turka. 2015. Control of PI(3) kinase in Treg cells maintains homeostasis and lineage stability. *Nature Immunology* 16: 188-196.
41. Hedrick, S. M., R. Michelini, A. L. Doedens, A. W. Goldrath, and E. L. Stone. 2012. FOXO transcription factors throughout T cell biology. *Nature Reviews Immunology* 12: 649-661.
42. Miyazaki, M., K. Miyazaki, S. Chen, M. Itoi, M. Miller, L. F. Lu, N. Varki, A. N. Chang, D. H. Broide, and C. Murre. 2014. Id2 and Id3 maintain the regulatory T cell pool to suppress inflammatory disease. *Nat Immunol* 15: 767-776.
43. Yang, C. Y., J. A. Best, J. Knell, E. Yang, A. D. Sheridan, A. K. Jesionek, H. S. Li, R. R. Rivera, K. C. Lind, L. M. D'Cruz, S. S. Watowich, C. Murre, and A. W. Goldrath. 2011. The transcriptional

regulators Id2 and Id3 control the formation of distinct memory CD8+ T cell subsets. *Nat Immunol* 12: 1221-1229.
44. Ouyang, W., W. Liao, C. T. Luo, N. Yin, M. Huse, M. V. Kim, M. Peng, P. Chan, Q. Ma, Y. Mo, D. Meijer, K. Zhao, A. Y. Rudensky, G. Atwal, M. Q. Zhang, and M. O. Li. 2012. Novel Foxo1-dependent transcriptional programs control T(reg) cell function. *Nature* 491: 554-559.
45. Madisen, L., T. A. Zwingman, S. M. Sunkin, S. W. Oh, H. A. Zariwala, H. Gu, L. L. Ng, R. D. Palmiter, M. J. Hawrylycz, A. R. Jones, E. S. Lein, and H. Zeng. 2010. A robust and high-throughput Cre reporting and characterization system for the whole mouse brain. *Nat Neurosci* 13: 133-140.
46. Couter, C. J., and N. K. Surana. 2016. Isolation and Flow Cytometric Characterization of Murine Small Intestinal Lymphocytes. *JoVE*: e54114.
47. Srivastava, S., M. A. Koch, M. Pepper, and D. J. Campbell. 2014. Type I interferons directly inhibit regulatory T cells to allow optimal antiviral T cell responses during acute LCMV infection. *J Exp Med* 211: 961-974.
48. Koch, M. A., G. Tucker-Heard, N. R. Perdue, J. R. Killebrew, K. B. Urdahl, and D. J. Campbell. 2009. The transcription factor T-bet controls regulatory T cell homeostasis and function during type 1 inflammation. *Nat Immunol* 10: 595-602.
49. Zaiss, D. M. W., and P. J. Coffer. 2018. Forkhead box transcription factors as context-dependent regulators of lymphocyte homeostasis. *Nat Rev Immunol* 18: 703-715.
50. Leenders, H., S. Whiffield, C. Benoist, and D. Mathis. 2000. Role of the forkhead transcription family member, FKHR, in thymocyte differentiation. *European journal of immunology* 30: 2980-2990.
51. Fruman, D. A., and C. Rommel. 2014. PI3K and cancer: lessons, challenges and opportunities. *Nature reviews. Drug discovery* 13: 140-156.
52. Dengler, H. S., G. V. Baracho, S. A. Omori, S. Bruckner, K. C. Arden, D. H. Castrillon, R. A. DePinho, and R. C. Rickert. 2008. Distinct functions for the transcription factor Foxo1 at various stages of B cell differentiation. *Nature Immunology* 9: 1388-1398.
53. Kerdiles, Y. M., D. R. Beisner, R. Tinoco, A. S. Dejean, D. H. Castrillon, R. A. DePinho, and S. M. Hedrick. 2009. Foxo1 links homing and survival of naive T cells by regulating L-selectin, CCR7 and interleukin 7 receptor. *Nature Immunology* 10: 176-184.
54. Ochodnicka-Mackovicova, K., M. Bahjat, C. Maas, A. van der Veen, T. A. Bloedjes, A. M. de Bruin, H. van Andel, C. E. Schrader, R. W. Hendriks, E. Verhoeyen, R. J. Bende, C. J. M. van Noesel, and J. E. J. Guikema. 2016. The DNA Damage Response Regulates RAG1/2 Expression in Pre–B Cells through ATM-FOXO1 Signaling. *The Journal of Immunology* 197: 2918-2929.
55. Vogt, P. K., H. Jiang, and M. Aoki. 2005. Triple layer control: phosphorylation, acetylation and ubiquitination of FOXO proteins. *Cell cycle (Georgetown, Tex.)* 4: 908-913.
56. Chow, K. T., G. A. Timblin, S. M. McWhirter, and M. S. Schlissel. 2013. MK5 activates Rag transcription via Foxo1 in developing B cells. *The Journal of Experimental Medicine* 210: 1621-1634.
57. Dominguez-Sola, D., J. Kung, A. B. Holmes, V. A. Wells, T. Mo, K. Basso, and R. Dalla-Favera. 2015. The FOXO1 Transcription Factor Instructs the Germinal Center Dark Zone Program. *Immunity* 43: 1064-1074.
58. Bupp, M. R., B. Edwards, C. Guo, D. Wei, G. Chen, B. Wong, E. Masteller, and S. L. Peng. 2009. T cells require Foxo1 to populate the peripheral lymphoid organs. *European Journal of Immunology* 39: 2991-2999.
59. Lee, J. H., S. G. Kang, and C. H. Kim. 2006. FoxP3+ T Cells Undergo Conventional First Switch to Lymphoid Tissue Homing Receptors in Thymus but Accelerated Second Switch to Nonlymphoid Tissue Homing Receptors in Secondary Lymphoid Tissues. *The Journal of Immunology* 178: 301-311.
60. Kerdiles, Y. M., E. L. Stone, D. L. Beisner, M. A. McGargill, I. L. Ch'en, C. Stockmann, C. D. Katayama, and S. M. Hedrick. 2010. Foxo Transcription Factors Control Regulatory T Cell Development and Function. *Immunity* 33: 890-904.
61. Arvey, A., J. van der Veeken, R. M. Samstein, Y. Feng, J. A. Stamatoyannopoulos, and A. Y. Rudensky. 2014. Inflammation-induced repression of chromatin bound by the transcription factor Foxp3 in regulatory T cells. *Nat Immunol* 15: 580-587.

62. Samstein, R. M., A. Arvey, S. Z. Josefowicz, X. Peng, A. Reynolds, R. Sandstrom, S. Neph, P. Sabo, J. M. Kim, W. Liao, M. O. Li, C. Leslie, J. A. Stamatoyannopoulos, and A. Y. Rudensky. 2012. Foxp3 Exploits a Pre-Existent Enhancer Landscape for Regulatory T Cell Lineage Specification. *Cell* 151: 153-166.
63. Corthésy, B. 2013. Multi-Faceted Functions of Secretory IgA at Mucosal Surfaces. *Frontiers in Immunology* 4: 185.
64. Koch, M. A., G. L. Reiner, K. A. Lugo, L. Kreuk, A. G. Stanbery, E. Ansaldo, T. D. Seher, W. B. Ludington, and G. M. Barton. 2016. Maternal IgG and IgA Antibodies Dampen Mucosal T Helper Cell Responses in Early Life. *Cell* 165: 827-841.
65. Jackson, S. W., N. E. Scharping, N. S. Kolhatkar, S. Khim, M. A. Schwartz, Q. Z. Li, K. L. Hudkins, C. E. Alpers, D. Liggitt, and D. J. Rawlings. 2014. Opposing impact of B cell-intrinsic TLR7 and TLR9 signals on autoantibody repertoire and systemic inflammation. *J Immunol* 192: 4525-4532.
66. Rowland, S. L., J. M. Riggs, S. Gilfillan, M. Bugatti, W. Vermi, R. Kolbeck, E. R. Unanue, M. A. Sanjuan, and M. Colonna. 2014. Early, transient depletion of plasmacytoid dendritic cells ameliorates autoimmunity in a lupus model. *Journal of Experimental Medicine* 211: 1977-1991.
67. Rodríguez-Borlado, L., D. F. Barber, C. Hernández, M. A. Rodríguez-Marcos, A. Sánchez, E. Hirsch, M. Wymann, C. Martínez-A, and A. C. Carrera. 2003. Phosphatidylinositol 3-Kinase Regulates the CD4/CD8 T Cell Differentiation Ratio. *The Journal of Immunology* 170: 4475-4482.
68. Witt, C. M., and E. A. Robey. 2004. The Ins and Outs of CCR7 in the Thymus. *The Journal of Experimental Medicine* 200: 405-409.
69. Kwan, J., and N. Killeen. 2004. CCR7 Directs the Migration of Thymocytes into the Thymic Medulla. *The Journal of Immunology* 172: 3999-4007.
70. Yin, X., E. Ladi, S. Chan, O. Li, N. Killeen, D. J. Kappes, and E. A. Robey. 2007. CCR7 Expression in Developing Thymocytes Is Linked to the CD4 versus CD8 Lineage Decision. *The Journal of Immunology* 179: 7358-7364.
71. Newton, R. H., S. Shrestha, J. M. Sullivan, K. B. Yates, E. B. Compeer, N. Ron-Harel, B. R. Blazar, S. J. Bensinger, W. N. Haining, M. L. Dustin, D. J. Campbell, H. Chi, and L. A. Turka. 2018. Maintenance of CD4 T cell fitness through regulation of Foxo1. *Nature immunology*.
72. Prinz, I., U. Klemm, S. Kaufmann, and U. Steinhoff. 2004. Exacerbated colitis associated with elevated levels of activated CD4+ T cells in TCRα chain transgenic mice. *Gastroenterology* 126: 170-181.
73. Brunet, A., A. Bonni, M. J. Zigmond, M. Z. Lin, P. Juo, L. S. Hu, M. J. Anderson, K. C. Arden, J. Blenis, and M. E. Greenberg. 1999. Akt promotes cell survival by phosphorylating and inhibiting a Forkhead transcription factor. *Cell* 96: 857-868.
74. Kops, G. J., N. D. de Ruiter, A. M. De Vries-Smits, D. R. Powell, J. L. Bos, and B. M. Burgering. 1999. Direct control of the Forkhead transcription factor AFX by protein kinase B. *Nature* 398: 630-634.
75. Staron, M. M., S. M. Gray, H. D. Marshall, I. A. Parish, J. H. Chen, C. J. Perry, G. Cui, M. O. Li, and S. M. Kaech. 2014. The Transcription Factor FoxO1 Sustains Expression of the Inhibitory Receptor PD-1 and Survival of Antiviral CD8+ T Cells during Chronic Infection. *Immunity* 41: 802-814.
76. Kim, M. V., W. Ouyang, W. Liao, M. Q. Zhang, and M. O. Li. 2013. The Transcription Factor Foxo1 Controls Central-Memory CD8+ T Cell Responses to Infection. *Immunity* 39: 286-297.
77. Delpoux, A., R. Michelini, S. Verma, C.-Y. Lai, K. D. Omilusik, D. T. Utzschneider, A. J. Redwood, A. W. Goldrath, C. A. Benedict, and S. M. Hedrick. 2017. Continuous activity of Foxo1 is required to prevent anergy and maintain the memory state of CD8+ T cells. *Journal of Experimental Medicine* 215.
78. Pearce, E. L., M. C. Poffenberger, C.-H. H. Chang, and R. G. Jones. 2013. Fueling immunity: insights into metabolism and lymphocyte function. *Science (New York, N.Y.)* 342: 1242454.
79. Scaduto, R. C., and L. W. Grotyohann. 1999. Measurement of Mitochondrial Membrane Potential Using Fluorescent Rhodamine Derivatives. *Biophysical Journal* 76: 469-477.
80. Wilhelm, K., K. Happel, G. Eelen, S. Schoors, M. F. Oellerich, R. Lim, B. Zimmermann, I. M. Aspalter, C. A. Franco, T. Boettger, T. Braun, M. Fruttiger, K. Rajewsky, C. Keller, J. C. Brüning, H. Gerhardt, P. Carmeliet, and M. Potente. 2016. FOXO1 couples metabolic activity and growth state in the vascular endothelium. *Nature* 529: 216.

81. Kim, S.-K., D. S. Reed, S. Olson, M. J. Schnell, J. K. Rose, P. A. Morton, and L. Lefrançois. 1998. Generation of mucosal cytotoxic T cells against soluble protein by tissue-specific environmental and costimulatory signals. *Proceedings of the National Academy of Sciences* 95: 10814-10819.
82. Kurts, C., W. R. Heath, F. R. Carbone, J. Allison, J. F. Miller, and H. Kosaka. 1996. Constitutive class I-restricted exogenous presentation of self antigens in vivo. *The Journal of Experimental Medicine* 184: 923-930.
83. Friesen, T. J., Q. Ji, and P. J. Fink. 2016. Recent thymic emigrants are tolerized in the absence of inflammation. *The Journal of Experimental Medicine* 213: 913-920.
84. Kakaradov, B., J. Arsenio, C. E. Widjaja, Z. He, S. Aigner, P. J. Metz, B. Yu, E. J. Wehrens, J. Lopez, S. H. Kim, E. I. Zuniga, A. W. Goldrath, J. T. Chang, and G. W. Yeo. 2017. Early transcriptional and epigenetic regulation of CD8(+) T cell differentiation revealed by single-cell RNA sequencing. *Nat Immunol* 18: 422-432.
85. Man, K., M. Miasari, W. Shi, A. Xin, D. C. Henstridge, S. Preston, M. Pellegrini, G. T. Belz, G. K. Smyth, M. A. Febbraio, S. L. Nutt, and A. Kallies. 2013. The transcription factor IRF4 is essential for TCR affinity–mediated metabolic programming and clonal expansion of T cells. *Nature Immunology* 14.
86. Nayar, R., E. Schutten, B. Bautista, K. Daniels, A. L. Prince, M. Enos, M. A. Brehm, S. L. Swain, R. M. Welsh, and L. J. Berg. 2014. Graded Levels of IRF4 Regulate CD8+ T Cell Differentiation and Expansion, but Not Attrition, in Response to Acute Virus Infection. *The Journal of Immunology* 192: 5881-5893.
87. Huber, M., and M. Lohoff. 2014. IRF4 at the crossroads of effector T-cell fate decision. *European Journal of Immunology* 44: 1886-1895.
88. Miyagawa, F., H. Zhang, A. Terunuma, K. Ozato, Y. Tagaya, and S. I. Katz. 2012. Interferon regulatory factor 8 integrates T-cell receptor and cytokine-signaling pathways and drives effector differentiation of CD8 T cells. *Proceedings of the National Academy of Sciences* 109: 12123-12128.
89. Yoshida, Y., R. Yoshimi, H. Yoshii, D. Kim, A. Dey, H. Xiong, J. Munasinghe, I. Yazawa, M. J. O'Donovan, O. A. Maximova, S. Sharma, J. Zhu, H. Wang, H. C. Morse, and K. Ozato. 2014. The Transcription Factor IRF8 Activates Integrin-Mediated TGF-β Signaling and Promotes Neuroinflammation. *Immunity* 40: 187-198.
90. Feng, J., H. Wang, D.-M. Shin, M. Masiuk, C.-F. Qi, and H. C. Morse. 2011. IFN Regulatory Factor 8 Restricts the Size of the Marginal Zone and Follicular B Cell Pools. *The Journal of Immunology* 186: 1458-1466.
91. Shukla, V., and R. Lu. 2014. IRF4 and IRF8: governing the virtues of B lymphocytes. *Frontiers in Biology* 9: 269-282.
92. Kallies, A., and K. L. Good-Jacobson. 2017. Transcription Factor T-bet Orchestrates Lineage Development and Function in the Immune System. *Trends in Immunology* 38: 287-297.
93. Lazarevic, V., L. H. Glimcher, and G. M. Lord. 2013. T-bet: a bridge between innate and adaptive immunity. *Nature reviews. Immunology* 13: 777-789.
94. Dominguez-Villar, M., and D. A. Hafler. 2018. Regulatory T cells in autoimmune disease. *Nat Immunol*.
95. Wohlfert, E. A., J. R. Grainger, N. Bouladoux, J. E. Konkel, G. Oldenhove, C. H. Ribeiro, J. A. Hall, R. Yagi, S. Naik, R. Bhairavabhotla, W. E. Paul, R. Bosselut, G. Wei, K. Zhao, M. Oukka, J. Zhu, and Y. Belkaid. 2011. GATA3 controls Foxp3(+) regulatory T cell fate during inflammation in mice. *J Clin Invest* 121: 4503-4515.
96. Kee, B. L. 2009. E and ID proteins branch out. *Nat Rev Immunol* 9: 175-184.
97. Quong, M. W., W. J. Romanow, and C. Murre. 2002. E protein function in lymphocyte development. *Annu Rev Immunol* 20: 301-322.
98. Omilusik, K. D., L. A. Shaw, and A. W. Goldrath. 2013. Remembering one's ID/E-ntity: E/ID protein regulation of T cell memory. *Curr Opin Immunol* 25: 660-666.
99. Miyazaki, M., R. R. Rivera, K. Miyazaki, Y. C. Lin, Y. Agata, and C. Murre. 2011. The opposing roles of the transcription factor E2A and its antagonist Id3 that orchestrate and enforce the naive fate of T cells. *Nat Immunol* 12: 992-1001.
100. Omilusik, K. D., M. S. Nadjsombati, L. A. Shaw, B. Yu, J. J. Milner, and A. W. Goldrath. 2018. Sustained Id2 regulation of E proteins is required for terminal differentiation of effector CD8(+) T cells. *J Exp Med* 215: 773-783.

101. Rauch, K. S., M. Hils, E. Lupar, S. Minguet, M. Sigvardsson, M. E. Rottenberg, A. Izcue, C. Schachtrup, and K. Schachtrup. 2016. Id3 Maintains Foxp3 Expression in Regulatory T Cells by Controlling a Transcriptional Network of E47, Spi-B, and SOCS3. *Cell Rep* 17: 2827-2836.
102. Rauch, K. S., M. Hils, A. J. Menner, M. Sigvardsson, S. Minguet, P. Aichele, C. Schachtrup, and K. Schachtrup. 2017. Regulatory T cells characterized by low Id3 expression are highly suppressive and accumulate during chronic infection. *Oncotarget* 8: 102835-102851.
103. Sun, I. H., M. H. Oh, L. Zhao, C. H. Patel, M. L. Arwood, W. Xu, A. J. Tam, R. L. Blosser, J. Wen, and J. D. Powell. 2018. mTOR Complex 1 Signaling Regulates the Generation and Function of Central and Effector Foxp3(+) Regulatory T Cells. *J Immunol*.
104. Gavin, M. A., S. R. Clarke, E. Negrou, A. Gallegos, and A. Rudensky. 2002. Homeostasis and anergy of CD4(+)CD25(+) suppressor T cells in vivo. *Nat Immunol* 3: 33-41.
105. Milner, J. J., C. Toma, B. Yu, K. Zhang, K. Omilusik, A. T. Phan, D. Wang, A. J. Getzler, T. Nguyen, S. Crotty, W. Wang, M. E. Pipkin, and A. W. Goldrath. 2017. Runx3 programs CD8(+) T cell residency in non-lymphoid tissues and tumours. *Nature* 552: 253-257.
106. Li, C., J. R. DiSpirito, D. Zemmour, R. G. Spallanzani, W. Kuswanto, C. Benoist, and D. Mathis. 2018. TCR Transgenic Mice Reveal Stepwise, Multi-site Acquisition of the Distinctive Fat-Treg Phenotype. *Cell*.